



A transition in atmospheric emissions of particles and gases from on-road heavy-duty trucks

Liyuan Zhou¹, Åsa M. Hallquist^{2*}, Mattias Hallquist³, Christian M. Salvador³, Samuel M. Gaita³, Åke Sjödin², Martin Jerksjö², Håkan Salberg², Ingvar Wängberg², Johan Mellqvist⁴, Qianyun Liu¹, Berto P. Lee¹, Chak K. Chan^{1*}

¹School of Energy and Environment, City University of Hong Kong, Hong Kong, China

²IVL Swedish Environmental Research Institute, Gothenburg, Sweden

³Department of Chemistry and Molecular Biology, University of Gothenburg, Gothenburg, Sweden

⁴Earth and Space Sciences, Chalmers University of Technology, Gothenburg, Sweden

Correspondence to: Åsa M. Hallquist (asa.hallquist@ivl.se), Chak K. Chan (Chak.K.Chan@cityu.edu.hk)

Abstract. The transition in extent and characteristics of atmospheric emissions caused by the modernisation of the heavy-duty on-road fleet were studied utilising roadside measurements. Emissions of particle number (PN), particle mass (PM), black carbon (BC), nitrogen oxides (NO_x), carbon monoxide (CO), hydrocarbon (HC), particle size distributions and particle volatility were measured from 556 individual heavy-duty trucks (HDTs). Substantial reductions in PM, BC, NO_x, CO and to a lesser extent PN were observed from Euro III to Euro VI HDTs by 99%, 98%, 93% and 57% for the average emissions factors of PM, BC, NO_x, and CO respectively. Despite significant total reductions in NO_x emissions, the fraction of NO₂ in the NO_x emissions increased continuously from Euro IV to Euro VI HDTs. Larger data scattering was evident for PN emissions in comparison to solid particle number (SPN) for Euro VI HDTs, indicating a highly variable fraction of volatile particle components. Particle size distributions of Euro III to EEV HDTs were bimodal, whereas those of Euro VI HDTs were nucleation mode dominated. High emitters disproportionately contributed to a large fraction of the total emissions with the highest-emitting 10% of HDTs in each pollutant category being responsible for 65% of total PM, 70% of total PN and 44% of total NO_x emissions, respectively. Euro VI HDTs, which accounted for 53% of total kilometres driven by Swedish HDTs, were estimated to only contribute to 2%, 6%, 12% and 47% of PM, BC, NO_x, and PN emissions. A shift to a Euro VI HDTs dominant fleet would promote a transition of atmospheric emissions towards low PM, BC, NO_x, and CO levels. Nonetheless, reducing PN, SPN, and NO₂ emissions from Euro VI HDTs is still important to improve air quality in urban environments.

1 Introduction

Vehicular emissions contribute significantly to gaseous and particle pollutants in the urban atmosphere and description of their extent and characteristics are key input components for urban air quality modelling. As technology and traffic demands change, so do the characteristics of the emissions. In Europe, the introduction of new legislation, especially Euro VI, has aimed to



30 reduce emissions of many pollutants. Legislation exists for particles (mass and number) and selected gases, however, there are
31 also many components of the emissions that are not directly regulated but are potentially detrimental to human health. The
32 most notable example of a non-regulated pollutant is the abundance of ultrafine particles (UFP) (Campagnolo et al., 2019),
33 defined as particles with a diameter less than 100 nm (Zhu et al., 2002). UFPs can cause lung disease, an increase of blood
34 coagulability and cardiovascular disease and related mortality (Du et al., 2016). In the most recent Euro class, this has partly
35 been covered by introducing a limit on the solid particle number (SPN) while volatile particles and particles less than 23 nm
36 are not considered. Furthermore, the legislation has mainly been based on test cycles performed before introducing a new
37 engine into the market but only recently also off-cycle and in-service conformity testing has been introduced, hence the actual
38 performance in real-traffic is less constrained, where driving pattern, maintenance, and age of engine will vary. Here real-
39 traffic studies may capture variability between vehicles and also put the effect of new legislation and parallel phase-out of
40 older technology into perspective for the abatement of urban air pollution.

41 Heavy-duty vehicles (HDVs) usually account for a smaller number fraction of on-road vehicles than light-duty vehicles
42 but they tend to contribute to a disproportionately high fraction of mobile source particulate matter emissions (Gertler, 2005;
43 Cui et al., 2017). Emissions from HDVs, often diesel, are significantly affected by the engine type, exhaust after-treatment
44 system (ATS), and driving conditions. The main purpose of ATS is the reduction of particulate and gaseous pollutants. Diesel
45 Oxidation Catalysts (DOC) are used for reducing hydrocarbon emissions, selective catalytic reduction (SCR) systems or
46 exhaust gas recirculation (EGR) are employed to mitigate NO_x emissions, and diesel particulate filters (DPF) can reduce
47 particulate matter mass emissions. The use of ATS can, however, bring undesired side effects. For example, conversion of SO₂
48 to SO₃ and increased gaseous sulfuric acid formation have been reported from DOCs (Arnold et al., 2012). DPFs potentially
49 enhance the formation of UFP (Herner et al., 2011; Preble et al., 2017). Retrofitted DPF can slightly reduce the NO_x emissions
50 but significantly increase the direct emission of NO₂ by as much as a factor of 8 (Smith et al., 2019). Failure of the temperature-
51 dependent SCR in eliminating the excess NO₂ leads to an elevated NO₂ to NO_x ratio (Herner et al., 2009; Bishop et al., 2010;
52 He et al., 2015).

53 The Euro standard regulates vehicle emission limits in Europe. The Euro III standard was established in 1999, and more
54 stringent Euro IV and Euro V standards were implemented in 2005 and 2008, respectively. The Enhanced Environmentally
55 Friendly Vehicle (EEV) is a voluntary environmental standard which lies between the levels of Euro V and Euro VI. The
56 currently enforced Euro VI standard has been implemented since 2013-2014 and introduced SPN limits into the regulation for
57 the first time. Generally, newer engines are expected to perform better in controlling pollutant emissions. Guo et al. (2014)
58 reported that Euro V diesel buses performed better than Euro IV and Euro III diesel buses in the emissions of all the pollutants,
59 except for the generation of more nucleation mode particles. The latest 2018 European Environmental Agency (EEA) report
60 confirms an overall improvement in the European air quality, while the road transport sector remains one of the major
61 contributors to pollutant emissions and the largest contributor to the total NO_x emission (Grigoratos et al., 2019; EEA, 2018).
62 A recent on-board sensor-based study pointed out that HDVs emitted more than three times the NO_x certification standard
63 during real-world hot-driving and idling operations (Tan et al., 2019). Published data regarding particle and gaseous pollutant



64 emissions from real-world on-road Euro VI heavy-duty vehicles are scarce and often limited by the small sample
65 size (Giechaskiel et al., 2018; Grigoratos et al., 2019; Moody and Tate, 2017). Remote sensing sampling can measure a large
66 sample size of vehicles but are usually restricted to gaseous pollutant emissions (Burgard and Provinsal, 2009; Burgard et al.,
67 2006; Carslaw et al., 2011). From an air quality perspective, the particle emissions are crucial. The complexity and dynamics
68 of atmospheric particles require detailed information of its emission for atmospheric modelling and for descriptions of their
69 health impacts. For example, particle size is important to determine the effects on respiratory deposition in
70 humans (Manigrasso et al., 2017; Lv et al., 2016).

71 Diesel exhaust particles are a complex mixture of numerous semi-volatile and non-volatile species, and the semi-volatile
72 compounds will experience gas-to-particle partitioning in the atmosphere (Robinson et al., 2007; Donahue et al., 2006). Biswas
73 et al. (2009) reported that the semi-volatile fraction in HDV emission is more oxidative than the refractory particles, which
74 may change the redox state in cells and cause oxidative stress. Semi-volatile organic compounds, such as PAHs and their
75 derivatives may possess genotoxic and carcinogenic characteristics (Bocchi et al., 2016; Vojtisek-Lom et al., 2015).
76 Giechaskiel et al. (2009) suggested using the volatile mass fraction as a metric to assess health effects as the volatile mass
77 dissolves in the lung fluid and thereby interacts with epithelial cells. Deploying a Volatility Tandem Differential Mobility
78 Analyzer in suburban Guangzhou, China, Cheung et al. (2016) found that 57–71 % of ambient particles between 40 and 300 nm
79 contain volatile components. Furthermore, the evaporated semi-volatile compounds from the particle phase can be further
80 oxidized to form secondary organic aerosols (SOA) (Hallquist et al., 2009; Gentner et al., 2017). To better quantify the health
81 effects and global and regional contributions of road traffic to the total particle burden in the atmosphere, information on the
82 volatility properties of vehicle particulate emissions is needed.

83 Different approaches have been applied to study the emissions from HDTs (Franco et al., 2013). Chassis dynamometer
84 tests provide relatively comprehensive emission characteristics of individual vehicles (Jiang et al., 2018; Chen et al., 2018;
85 Thiruvengadam et al., 2015), but the artificial driving cycles make it difficult to simulate the full range of real-world driving
86 conditions. Portable emission measurement systems (PEMS) (Grigoratos et al., 2019; Pirjola et al., 2017) and plume chasing
87 studies (Lau et al., 2015; Pirjola et al., 2016) have been conducted in real-world environments but are often limited by small
88 sample sizes. Tunnel studies (Li et al., 2018) measure the average emission of all vehicles passing through the tunnel without
89 specific emission information of vehicle types. Roadside measurements, as presented in this study, provide an opportunity to
90 study real-world on-road traffic emissions on large sample sizes with individual vehicle information (e.g. Hallquist et al., 2013;
91 Dallmann et al., 2012; Carslaw and Rhys-Tyler, 2013; Watne et al., 2018).

92 In this work, we measured the gaseous and particle emissions from 556 on-road individual HDTs and quantified changes
93 in emissions and the potential transition in characteristics caused by the reduction achieved by the introduction of more
94 stringent Euro standards. Particle size distributions and particle volatilities were investigated with respect to Euro class, and
95 pollutant emission characteristics were studied with respect to year of registration. Cumulative pollutant distributions were
96 established to demonstrate the importance of controlling high-emitters in reducing total emissions. The typical contribution of
97 air pollution emissions from each Euro class HDTs was estimated based on total vehicle kilometres driven. Results of the



98 presented pollutant emission factors in our study will be useful for both emission models and emission inventories. A clear
99 transition of atmospheric pollutant emission trends was evident and can provide useful guidance for policies regarding the
100 regulation of existing fleets.

101 **2 Methods**

102 **2.1 Field sampling site**

103 Pollutant emissions from HDTs were measured at a roadside location in Gothenburg, Sweden (Fig. 1). The HDTs passed the
104 sampling location with an average speed of 27 km h^{-1} and acceleration of $0.7 \text{ km h}^{-1} \text{ s}^{-1}$ on a slight uphill slope ($\sim 2^\circ$).

105 **2.2 Air sampling**

106 The sampling of the emissions was conducted in line with Hallquist et al. (2013), i.e. extractive sampling of passing HDT
107 plumes. Air was continuously drawn through a flexible copper tube to the instruments inside a container. A similar
108 experimental set-up was previously applied to on-road bus emission measurements (Liu et al., 2019). Particles were measured
109 by an EEPS (Engine Exhaust Particle Sizer, Model 3090 TSI Inc.) in the size range of 5.6-560 nm with high time resolution
110 (10 Hz) while total particle number was measured by a butanol-based condensation particle counter (CPC Model 3775 TSI
111 Inc., 50 cut-off diameter 4 nm). Particle numbers measured by the two instruments showed a good correlation ($R^2=0.73$)
112 (Fig. S1). A second EEPS measured the outflow of a TD (thermodenuder, Dekati, Inc.), enabling estimations of particle
113 volatility. The data were corrected for size-dependent losses in the TD. The temperature inside the TD heating zone was set to
114 250°C with a residence time of $\sim 0.6 \text{ s}$, which is generally sufficient to evaporate nearly all the organics and sulphates from
115 the particles (Huffman et al., 2008). However, organics with extremely low volatility (organic saturation mass concentration,
116 $C^* < 10^{-5} \mu\text{g m}^{-3}$ at 298 K) may still be retained even at this high temperature (Gkatzelis et al., 2016). Thus, in this study, we
117 define the ‘non-volatile components’ as particle components that remain after passing through the TD operating at 250°C .
118 Differences in counting efficiencies between the two EEPS were accounted for by size-dependent correction factors (typically
119 less than 10%), which were retrieved by simultaneous sampling of ammonium sulphate particles by both EEPS and direct
120 comparison of their measured size distributions (Fig. S2). BC and the mixture of BC and brown carbon (BrC) were measured
121 by an Aethalometer at 880 nm and 370 nm respectively (Model AE 33, Magee Scientific Inc.). The determination of particle
122 mass concentrations by the integrated particle size distribution (IPSD) method requires information on particle density. Particle
123 sphericity and unit density were assumed due to a lack of detailed knowledge about the chemical composition of the emitted
124 particles. Figure S3 shows that there is a good linear relationship between the BC mass measured by the Aethalometer and the
125 non-volatile particle mass measured by the EEPS but assuming sphericity and unit density the EEPS mass is lower, which
126 indicates a potential underestimation of the effective non-volatile particle density. There have been several studies on the
127 morphology and density of combustion generated particles and its detailed dependence on combustion and dilution condition



128 (e.g. Maricq and Ning, 2004; Ristimaki et al., 2007; Liu et al., 2009; Zheng et al., 2011; Quiros et al., 2015). However, to be
129 consistent, avoid assumptions and to compare with a majority of previously reported data, unity density was used for further
130 discussion and comparisons. CO₂ was measured by a non-dispersive infrared gas analyser (LI-840, LI-COR Inc.). NO_x and
131 NO were measured simultaneously by two separate chemiluminescent analysers (Model 42i, Thermo Scientific Inc.), and the
132 NO₂ concentration was calculated from the difference between the NO_x and NO concentrations. SO₂ was measured by a pulsed
133 fluorescence gas analyser (Model 43c, Thermo Scientific Inc.). A Remote Sensing Device (RSD) (OPUS Inspection Inc.) was
134 used to measure the gaseous emission factors of CO, NO_x, and HC. Briefly, the instrument was set up with a transmitter and a
135 receiver on the same side of the truck passing lane and a reflector on the opposite side. Co-linear beams of IR and UV light
136 are emitted and cross-reflected through the plume and light attenuation related to respective pollutant concentrations are
137 measured. Gas pollutant concentrations were determined relative to CO₂ as measured by the RSD. NO_x and NO measured by
138 the gas analysers and the RSD were in agreement ($R^2=0.53$ and 0.66 respectively, Figs. S4, S8a). The High-Resolution Time-
139 of-Flight Chemical Ionization Mass Spectrometer (HR-ToF-CIMS) shown in Fig. 1 was used to characterise the chemical
140 composition of organic and inorganic compounds in the gas and particle phase, emitted from the HDTs. However, the extensive
141 chemical characterisation is beyond the scope of this work and will be presented elsewhere.

142 All the instruments were operated at least at 1 Hz of sampling frequency to capture rapidly changing concentrations during
143 the passage of a HDT. A camera at the roadside recorded the HDT plate numbers, which was used for identification and to
144 obtain engine Euro type information. A schematic of the experimental setup is given in Fig. 1 along with some examples of
145 typical temporal profiles of pollutant concentrations in the plumes from Euro III and Euro VI HDTs. In general, the duration
146 of a peak was around 5 s, for NO_x slightly longer, limiting measurements of high-frequency passages. Euro III HDTs typically
147 emitted a significant amount of PN, PM, NO_x, and non-volatile components (Fig. 1c). More than 95% of Euro III, Euro IV,
148 Euro V, and EEV HDTs had measurable particle emission signals. Significant differences in low particle and gaseous emissions
149 were evident for Euro VI HDTs (Fig. 1d and e).

150 **2.3 Data analysis**

151 The exact time of individual HDTs passing the sampling inlet was determined from the camera recordings and the associated
152 plume pollutant concentrations were integrated to calculate corresponding pollutant emission factors of individual HDTs as
153 described by Hallquist et al. (2013). Emissions of gases and particles from individual HDTs were normalized by the CO₂
154 concentration to compensate for different degrees of dilution during sampling (Janhäll and Hallquist (2005)). CO₂ peak
155 concentrations exceeding four times the standard deviation of the background signal were used as the base criterion for
156 successful plume capture. Peaks in NO_x, PN, PM, and BC concentrations concurrent with that of CO₂ signify the presence of
157 co-emitted pollutants in a HDT plume. Emission factors (EFs) of gaseous and particle emissions for individual HDTs can then
158 be expressed in units of amount of pollutant emitted per kg fuel burned based on the carbon balance method (Ban-Weiss et al.,
159 2009; Hak et al., 2009):



160
$$EF_{pollutant} = \frac{\int_{t_1}^{t_2} ([pollutant]_t - [pollutant]_{t_1}) dt}{\int_{t_1}^{t_2} ([CO_2]_t - [CO_2]_{t_1}) dt} \times EF_{CO_2}, \quad (1)$$

161 where $EF_{pollutant}$ is the emission factor of the respective pollutant. The time interval of t_1 to t_2 represents the period when the
162 instruments measured the concentration of an entire pollutant peak from an individual HDT (see Fig. 1c-e).
163 $\int_{t_1}^{t_2} ([pollutant]_t - [pollutant]_{t_1}) dt$ and $\int_{t_1}^{t_2} ([CO_2]_t - [CO_2]_{t_1}) dt$ are the changes in concentration of a pollutant and CO_2
164 during this time interval. EF_{CO_2} of $3158 \text{ g (kg diesel fuel)}^{-1}$ was used as the emission factor of CO_2 , assuming complete
165 combustion and a carbon content of 86.1% as given in Edwards et al. (2014). Emission factors for plumes with pollutant
166 concentrations lower than our set detection limit (four times the standard deviation of the pollutant background signal) were
167 replaced by the minimum value among all recorded emission factors (EF_{min}) rather than being omitted to avoid overestimating
168 emissions from low-emitting HDTs.

169 3 Results and Discussion

170 3.1 Fleet compositions

171 A total of 675 resolved plumes from 556 individual HDTs for the carriage of goods with weights exceeding 12 tonnes were
172 identified. There were 330 Swedish HDTs with Euro type information, 46 Swedish HDTs from which Euro type information
173 was not available, and 180 foreign licensed non-Swedish HDTs. Among the 330 Swedish trucks, Euro III, Euro IV, Euro V,
174 EEV, and Euro VI HDTs accounted for 3%, 5%, 30%, 5%, and 57%, respectively (Fig. S5).

175 3.2 Emissions variability

176 Differences in operating and ambient conditions may lead to differences in pollutant emission factors for the same HDT. In
177 this study, we utilized measurement data from 55 HDTs which passed the sampling location repeatedly, yielding a total of 137
178 plumes. The average pollutant emission factors of each HDT plotted against the individual plume measurements of the
179 corresponding HDT are shown in Fig. S6. In general, the emission factors of PM, non-volatile PN, and NO_x showed little
180 variation ($R^2 \geq 0.77$) among multiple passages of the same HDT, however, higher variability was observed in the PN emissions.
181 This is likely related to variations in the formation of nucleation mode particles from volatile compounds which is more
182 sensitive to driving (Zheng et al., 2014) and dilution conditions. In the following discussion, for HDTs with multiple passages,
183 the average pollutant emission factors of all the detected plumes were used for that individual HDT.

184 3.3 Emissions factors (EFs) of particles and gaseous pollutants

185 Figure 2 a and b show the box-and-whisker plots of PM and PN emission factors (EFs) for different Euro classes. Generally,
186 both PM and PN emissions decreased with more stringent Euro emission standards, and especially for Euro VI where larger
187 changes in emission characteristics were evident. Using Euro III HDTs (median $EF_{PM} = 586 \text{ mg (kg fuel)}^{-1}$) as a baseline, the



188 median EF_{PM} for Euro IV, Euro V, EEV, and Euro VI HDTs have been reduced by 78.1%, 86.1%, 88.9%, and 99.8%
189 respectively. In particular, Euro VI HDTs has a median EF_{PM} of only 1.4 mg (kg fuel)⁻¹ (Fig. 2a). While it is noted that Euro
190 III to Euro VI standard certifications are based on chassis dynamometer cycle measurements, the Euro VI regulations have
191 started to include additional off-cycle and in-service conformity testing. The Euro emission standard of transient testing for
192 heavy-duty engines gives emission limits as brake specific emission factors, as mass (g) or number (#) of a specific pollutant
193 per kWh. In order to enable a comparison with the Euro emission standard, the EFs in g (or #) per kg fuel were converted using
194 a brake specific fuel consumption (BSFC) of 231.5 g kWh⁻¹. This is the average value for the long haul and regional delivery
195 cycles of chassis dynamometer tests of a typical rigid Euro VI truck (Rexeis et al., 2018). The uncertainty of the BSFC for
196 different Euro class HDTs operating over a wide range of engine conditions is generally within 25% (Mahmoudzadeh Andwari
197 et al., 2017; He et al., 2017; Dreher and Harley, 1998; Heywood, 1988). Note that our measurements represent points of time
198 similar to those in a cycle where the particle emissions can be most prominent. Looking at a whole cycle, this value will be
199 averaged, hence the results from our instantaneous plume measurements may represent an upper limit of the emissions. In Fig.
200 2a, the right y-axis gives the EFs converted into units of g kWh⁻¹ and the Euro standards are shown as blue crosses.

201 In general, the measured median EF_{PM} are lower than the Euro standards for all HDT types. In particular, the median
202 EF_{PM} for Euro VI HDTs is more than one order of magnitude lower than the Euro standard regulation value since Diesel
203 Particulate Filters (DPFs) are required for these Euro VI HDTs to comply with PM and PN standards (Williams and Minjares,
204 2016). The effectiveness of DPF in reducing particle emissions have been confirmed by various studies (Martinet et al., 2017;
205 May et al., 2014; Mendoza-Villafuerte et al., 2017; Moody and Tate, 2017; Preble et al., 2015). For example, Bergmann et al.
206 (2009) illustrated that post-DPF PM concentrations decreased by 99.5% compared with pre-DPF for the New European Driving
207 Cycle (NEDC). In real-world measurements, at least ~90% reductions in PM emissions compared to typical pre-DPF levels
208 have been reported (Bishop et al., 2015). Euro emission standards for PM of Euro IV and Euro V heavy-duty diesel engine are
209 the same, while the measured median EF_{PM} of the Euro V fleet was around 1.5 times lower than that of the Euro IV fleet. The
210 control of diesel engine emissions typically requires a compromise between NO_x and particle emission reduction (Clark et al.,
211 1999). The NO_x emission standard is more stringent for Euro V compared to Euro IV (a factor of 43% lower), and hence Euro
212 V HDTs are generally equipped with SCR or EGR to reduce NO_x. In contrast, Euro IV engines are rarely equipped with NO_x
213 after-treatment systems and thus must achieve the NO_x emission limits by tuning the engine performance parameters at the
214 expense of higher PM emissions (Preble et al., 2018; Van Setten et al., 2001). In each of the Euro III, Euro IV, Euro V, and
215 EEV classes, 25-50% of all the measured HDTs had an EF_{PM} higher than their corresponding Euro standards. As described
216 previously, this comparison with the Euro standard is relative and indicative. The higher emissions from individual HDTs may
217 indicate deterioration of engine performance due to wear caused by aging, mileage accumulation, or inadequate maintenance.
218 Our study shows that Euro VI HDTs generally have low PM emissions, but HDTs from older Euro classes frequently exceeded
219 their PM emission limits, suggesting that improved maintenance and suitable retrofitting of older engines are needed.

220 For PN emissions, EF_{PN} shows an overall trend similar to EF_{PM} . However, large data scatter was evident for Euro VI
221 HDTs, likely due to the sensitivity of nucleation mode particle formation to changes in driving conditions (Fig. 2b). Zheng et



222 al. (2014) reported high concentrations of nucleation mode particles under uphill driving conditions but low concentrations
223 under cruise and downhill driving conditions. It is important to note that the median EF_{PN} of Euro VI HDTs was significantly
224 lower than those from the other Euro type HDTs, which indicates efficient PM removal by the DPF without compromising on
225 total PN emission. Nonetheless, the decrease of particle number in the accumulation mode removes particle surface area
226 available for condensation and therefore favours nucleation of organics from fuel and lubrication oil. Le Breton et al. (2019)
227 confirmed the contribution of lubrication oil in bus emissions. Besides, DPFs can act as a sulphur reservoir and when excess
228 sulphur is released, SO_2 to SO_3 conversion can take place once the after-treatment temperature reaches a critical level (Herner
229 et al., 2011). In this case, total particle number emissions can increase due to nucleation from gas-phase sulphuric acid. Since
230 the fuel sulphur content is low, more than 90% of Euro VI HDTs had an EF_{SO_2} lower than the threshold in this study, organics
231 would play a more important role in the formation of nucleation mode particles.

232 Figure 2c shows that the median EF_{BC} was reduced by more than 99% for Euro VI HDTs compared to Euro III HDTs,
233 and the median EF_{BC} of Euro VI HDTs was even at the threshold ($0.2\text{mg}(\text{kg fuel})^{-1}$). The BC emissions generally showed an
234 overall decrease when moving towards newer Euro classes, which is similar to the EF_{PM} trend with the exception of Euro IV
235 HDTs. Compared with Euro V HDTs, the median EF_{BC} of Euro IV HDTs is 35% lower, however, the emission of the mixture
236 of BC and BrC from Euro IV HDTs is higher (Fig. S7a). Euro IV HDTs had the highest BrC contribution to the total light-
237 absorbing substances among all the Euro classes (Fig. S7b). Compared to the EEPs, the detection limit of the Aethalometer is
238 five times higher, which may influence the correlation between BC and PM at low mass loading conditions (Fig. S3).

239 Figure 2d compares the emissions of NO_2 and NO_x from different Euro class HDTs. The vertical lines represent the
240 different Euro standards. HDTs with either EF_{NO_2} or EF_{NO_x} lower than the detection limits of the instruments were removed
241 from the figure. In general, Euro VI HDTs exhibit more than 90% reduction in both median and average EF_{NO_x} compared to
242 Euro III HDTs. This is consistent with Carslaw et al. (2011) who estimated a 93% NO_x reduction from Euro III to Euro VI for
243 heavy goods vehicles (HGV) in the United Kingdom. Relatively, the Euro V HDTs had a larger fraction exceeding its Euro
244 standard, which may be due to the combined effects of poor engine tuning and the inactivity (low temperature) or deterioration
245 of SCR systems. Newer engines tend to exhibit a higher NO_2 emission fraction at a similar NO_x level, and the Euro VI HDTs
246 show a relatively low median EF_{NO_2} with a large range of data scatter and several high emitters. A continuous increase of
247 EF_{NO_2}/EF_{NO_x} was evident from Euro IV to Euro VI HDTs (Fig. S8b). This trend is consistent with Kozawa et al. (2014), who
248 reported an increase in the share of NO_2 to total NO_x from Euro III to Euro V vehicles. Euro VI HDTs have a higher NO_2
249 fraction because the DOC upstream of the filter is used to convert NO to NO_2 to control the soot loading in the DPF and
250 facilitate the passive regeneration (Van Setten et al., 2001). A failure of the NO_2 reduction due to the inactivity of the SCR,
251 resulting from low exhaust gas temperature, may result in a higher NO_2 emission (Bishop et al., 2010; Heeb et al., 2010; Herner
252 et al., 2009; May et al., 2014; Thiruvengadam et al., 2015). A more significant decrease in NO_x than NO_2 emissions of Euro
253 VI HDTs may cause an increase of EF_{NO_2}/EF_{NO_x} .

254 Compared with non-Swedish HDTs, Swedish HDTs generally have lower EFs in terms of all the pollutants (Fig. 2 and
255 Tables 1 and 2), which may be attributed to the more stringent domestic goals regarding pollution, clean air, greenhouse gas



256 emissions, energy efficiency, and innovative sustainable solutions (Government Offices of Sweden, 2017). One may note that
257 the non-Swedish HDTs was not identified according to Euro class and could contain a larger share of non-Euro VI trucks.

258 Table 1 compares the average emission data of PM and PN of the current work with previous studies according to the
259 HDT type and gives information on used measurement methods and driving conditions. Generally, the EF_{PM} and EF_{PN} in this
260 study are within the reported ranges of HDV emissions in the literature. Our estimated EF_{PM} of Euro III HDTs are comparable
261 to those of Euro III buses in Hallquist et al. (2013) and Pirjola et al. (2016). HDTs and buses within the same Euro class emit
262 similar amounts of PM. Watne et al. (2018) show that DPF retrofitted Euro III buses have much lower particle EFs. While
263 EF_{PM} is highly dependent on driving conditions such as speed and acceleration, the average EF_{PM} of Euro IV, Euro V and EEV
264 HDTs of this study: 172, 146, and 78 mg (kg fuel)⁻¹, respectively, are comparable to trends in previous studies (Hallquist et al.,
265 2013; Pirjola et al., 2016; Watne et al., 2018). Average EF_{PM} of Euro VI HDTs (5 mg (kg fuel)⁻¹/ 1.1 mg km⁻¹) is within the
266 range of emissions from HDVs with DPFs, e.g., 0.6 - 20.5 mg km⁻¹ for a recent chassis dynamometer test (Jiang et al., 2018)
267 and 2.5 - 8.7 mg km⁻¹ for road measurements in California (Quiros et al., 2016). Note that size ranges and measurement
268 methodologies may differ among the studies as listed in Table 1. Since most of the particle emissions related to road traffic
269 combustion are below 560 nm (Fig. 4), the size range in our study is comparable to most other wider range PM measurements.
270 Larger particles from road measurements of total PM may include non-combustion-related particles, e.g. resuspended road
271 dust, tire and brake particles, and should be interpreted with caution. In contrast to EF_{PM} , a much less obvious decrease in
272 average EF_{PN} was observed across different Euro classes. The reason for the high average particle emission for EEV and Euro
273 VI is likely due to high emissions of nucleation mode particles from a number of HDTs.

274 In Figure 3a, EF_{PM} and EF_{PN} of individual HDTs in this study and selected previous studies are plotted. HDTs with either
275 EF_{PM} or EF_{PN} lower than the detection limits of the instruments (0.07 mg (kg fuel)⁻¹ and 2.8×10^{11} # (kg fuel)⁻¹ respectively)
276 were removed from the figure (24% of the data). Generally, both EF_{PM} and EF_{PN} exhibited a decreasing trend from Euro III to
277 Euro IV and from Euro V to EEV HDTs. Overall, Euro VI HDTs had drastically lower PM emissions but highly scattered PN
278 emissions. Older Euro type buses retrofitted with DPF were shown to have reduced particle emissions, and some retrofitted
279 Euro III buses (black open triangles in Fig. 3a) may perform as well as Euro VI HDTs, indicating the effectiveness of
280 retrofitting older HDTs.

281 In more recent Euro standards, PN regulation has been introduced. The SPN as defined by the European Particle
282 Measurement Program (PMP) is the number of particles which remain after passing through an evaporation tube with a wall
283 temperature of 300-400°C (Zheng et al., 2011). The PMP only measures and regulates solid particles with a diameter larger
284 than 23 nm because measurements of smaller particles in the nucleation mode have poor repeatability (Martini et al., 2009).
285 SPN larger than 23 nm was integrated into the European emission regulation in 2013 for Euro VI heavy-duty
286 engines (Giechaskiel et al., 2012). A potential issue of evaporation measurements is that a fraction of the sub-23 nm particles
287 can also be formed downstream of the European PMP methodology through re-nucleation of semi-volatile precursors (Zheng
288 et al., 2012; Zheng et al., 2011). In our study, the TD temperature of 250°C is lower than the maximum temperature used by
289 the PMP (300-400°C) and does not follow the exact operation specifications of the PMP. However, Amanatidis et al. (2018)



290 summarised that TD is a suitable alternative approach for the removal of volatile particles. Particles larger than 23 nm
291 downstream of the TD were measured by the EEPS and we integrated the size bins from 23.5 nm to 560 nm to represent the
292 SPN. Figure 3b compares the EF_{PM} and EF_{SPN} of Euro VI HDTs. Generally, after-treatment control systems could not reduce
293 SPN emissions as effectively as PM emissions, indicating that more control of SPN emission of Euro VI HDTs may be
294 necessary.

295 Shown in Table 2 are the average EFs of gaseous pollutants (NO_x , CO, HC) in this study compared with other studies.
296 EF_{NO_x} generally decreased from the Euro III ($43.3 \text{ g (kg fuel)}^{-1}$) to Euro VI ($3.1 \text{ g (kg fuel)}^{-1}$) class, and are in good agreement
297 with reported values for HDTs in the literature. EF_{NO_x} of Euro III HDTs is moderately higher in this study. Note that the EF_{NO_x}
298 and EF_{PM} of EEV were much higher in Pirjola et al. (2016), in which only a limited number (3-4) vehicles were tested and
299 hard braking was common in approaching a 90° turn before accelerating again. The ratio of EF_{NO_2} to EF_{NO_x} generally agrees
300 with the projection in Kousoulidou et al. (2008) and on-road plume chasing measurements in Lau et al. (2015), while the ratio
301 is lower for the older Euro class HDTs compared with the remote sensing study in the UK (Carslaw and Rhys-Tyler, 2013).
302 Carslaw et al. (2019) reported a decreasing trend of EF_{NO_2}/EF_{NO_x} with vehicle mileage for Euro 6 light-duty diesel vehicles,
303 while no significant trend was identified for Euro VI HDTs in this study. There may be other parameters influencing the NO_x
304 emission. For example, Ko et al. (2019) reported that the NO_x emissions from Euro VI diesel vehicles were 29% higher in a
305 traffic jam than in smooth traffic conditions. The temperature of the exhaust and DPF regeneration may also influence the
306 EF_{NO_x} .

307 Compared with EF_{NO_x} , EF_{CO} decreased less pronounced from Euro III to Euro VI HDTs (57%). Compared with newer
308 Euro class HDTs, a larger fraction of HDTs in older Euro classes have an EF_{CO} exceeding the Euro standards, which indicates
309 that engine deterioration may have a serious effect on the CO emissions (Fig. S8c). Hallquist et al. (2013) reported a positive
310 relationship between EF_{CO} and EF_{PM} , i.e. high CO indicates incomplete combustion which favors soot formation. DPFs may
311 also reduce CO in addition to PM (Hallquist et al., 2013), which is in agreement with the lowest CO emission of 15.5 g (kg
312 fuel)^{-1} observed for DPF equipped Euro VI HDTs in this study. HC emission was relatively low for all HDT types, but no
313 obvious decreasing trend was evident for EF_{HC} from Euro III to Euro VI HDTs (Fig. S8d and Table 2). This does not reflect
314 the more stringent Euro standard limit regarding HC where the Euro VI limit is more than a factor of three lower than the
315 preceding Euro V/IV standards.

316 The 46 Swedish HDTs without available Euro type information emitted similar levels of particle and gaseous pollutants
317 to Euro VI HDTs and were thus likely equipped with newer Euro engines.

318 **3.4 Size-resolved EF_{PN} of volatile and non-volatile particles**

319 Figure 4 shows the average size-resolved number emission factors (solid lines) simultaneously measured via the bypass and
320 TD lines for different Euro class HDTs. The EF_{PN} of the volatile components is calculated as the difference of EF_{PN} measured
321 after the bypass line and the non-volatile component EF_{PN} measured after the TD line. To differentiate between nucleation and
322 accumulation mode particles, a cut point particle diameter of 30 nm was used as defined by Kittelson et al. (2002). In general,



323 all Euro III, Euro IV, Euro V and EEV HDTs showed a bimodal particle number size distribution, with one mode peaking at
324 ~6-10 nm (nucleation mode) and another at ~50-80 nm (accumulation/soot mode) (Maricq, 2007). For Euro VI HDTs the
325 particle number size distributions were dominated by the nucleation mode. The EF_{PN} of the accumulation mode particles
326 showed a decreasing trend from Euro III to EEV and for the Euro VI HDTs the accumulation mode was insignificant. For
327 heavy-duty diesel engines without a particulate filter, nucleation mode particles are mainly formed from organics. For vehicles
328 with DPF both organics and the fuel sulphur content influence the formation of nucleation mode particles (Vaaraslahti et al.,
329 2004). Thiruvengadam et al. (2012) found a direct relationship between exhaust nanoparticles in the nucleation mode and the
330 exhaust temperature of the DPF-SCR equipped diesel engine. These factors lead to high variability in the nucleation mode
331 fraction of EF_{PN} . Most particles in the nucleation mode evaporate after passing through the TD. Sakurai et al. (2003b) reported
332 that volatile compounds in diesel particles are mainly comprised of unburned lubrication oil.

333 The non-volatile components in the nucleation mode may consist of metallic ash from lubrication oil or fuel
334 additives (Sakurai et al., 2003a) or some organic compounds of extremely low volatility (Gkatzelis et al., 2016). In the
335 accumulation mode, the particle mode diameter shifted towards lower sizes after passing the TD. In Fig. 4, we also present the
336 median size distribution (dashed lines). There is a small difference between mean and median size distributions in the
337 accumulation mode while a bigger difference occurs in the nucleation mode. The latter mode is more dynamic and there are
338 larger possibilities for extreme values skewing the averages.

339 To be consistent with previous studies which overwhelmingly report average size distributions, we choose to utilize the
340 average size distributions for the discussions below. The volatilities of particle emissions in the accumulation and nucleation
341 mode have been evaluated by calculating the average EF_{PN} and EF_{PM} fraction remaining (after heating) of particles emitted
342 from Euro III-VI HDTs (Fig. S9). In general, the EF_{PN} fraction remaining in the nucleation mode was lower than that in the
343 accumulation mode across all HDTs in all Euro classes. In terms of particle mass, the nucleation mode and accumulation mode
344 showed similar EF_{PM} fractions remaining from Euro III to EEV HDTs, while Euro VI HDTs had a much lower EF_{PM} fraction
345 remaining in the nucleation mode than in the accumulation mode. Compared with other Euro class HDTs, Euro VI HDTs had
346 the lowest EF_{PN} and EF_{PM} fraction remaining in both nucleation and accumulation mode. Around 94% of the particles by
347 number and 55% of the particles by mass (or volume) in total were evaporated. Alföldy et al. (2009) reported that if the same
348 amount of volatile mass in the nucleation mode and accumulation mode were inhaled, 48% and 29% of the mass would deposit
349 in the lung respectively, implying that volatile mass in the nucleation mode would exert a 1.5 times stronger effect.

350 **3.5 Emissions from high emitters**

351 Figure 5 shows the cumulative emission distributions for PM, PN, NO_x and NO_2 emissions, with HDTs ranked in order from
352 dirtiest to cleanest. The plots show a significant skewedness towards a small fraction of HDTs with a high fraction of total
353 emissions (deviation from 1:1 line) for each pollutant, indicating the importance of “high emitters”. The disproportionate
354 skewed distribution of pollutants is a common feature of on-road emission measurements (Preble et al., 2018; Preble et al.,
355 2015; Dallmann et al., 2012). The highest-emitting 10% of HDTs in each pollutant were responsible for 65% of total PM, 70%



356 of total PN, 44% of total NO_x emissions and 69% of total NO₂, respectively. The distribution of NO_x has the least skewedness
357 compared with the other pollutants. If the 10% highest emitters for each pollutant were removed, the corresponding average
358 EF for PM, PN, NO_x, and NO₂ would decrease by 62%, 67%, 38%, and 66% respectively. However, the high emitters for each
359 pollutant are different. For example, Euro III HDTs account for 70% and 67% of the top 3% emitters for PM and BC emissions,
360 while Euro VI HDTs account for 80% and 56% of the top 3% emitters for PN and NO₂ emissions. Here, top 3% emitters were
361 chosen as the reference because Euro III HDTs only accounted for 3% of the total number of HDTs. Lau et al. (Lau et al.,
362 2015) similarly reported that not all high-emitters were members of the lower Euro classes and that high-emitters for a
363 particular pollutant may not simultaneously be high-emitters for other pollutants.

364 3.6 Fleet characteristics

365 Figure 6a-d show the changes in average EFs of PM, PN, BC, and NO_x with respect to the registration year of the HDTs.
366 Triennial average EFs were calculated, with truck registration years divided into 5 bins (2002-2005, 2006-2008, 2009-2011,
367 2012-2014 and 2015-2017). The black arrows in Fig. 6d show the years that the particular type of HDTs examined in this study
368 was first registered. Coupled with the possible phase-out of older fleets, the HDTs with more advanced engines gradually
369 accounted for a higher proportion of the total fleet. There is a significant improvement during the last years and the transition
370 to widespread adoption of Euro VI will take real-world on-road emissions into a new era of much lower contributions to air
371 pollution.

372 To estimate for each Euro class the typical contribution of air pollution emissions we utilised the number of kilometres
373 driven by HDTs on Swedish roads. During 2018, 4.1×10^9 and 9.2×10^8 kilometres were driven by Swedish and non-Swedish
374 diesel HDTs on Swedish roads, contributing to 82% and 18% to the total distances travelled by diesel HDTs respectively (Fig.
375 7a). The numbers of kilometres driven by Swedish Euro 0, Euro I, Euro II, Euro III, Euro IV, Euro V and Euro VI diesel HDTs
376 were 2.8×10^7 , 5.0×10^6 , 5.4×10^7 , 2.0×10^8 , 3.1×10^8 , 1.3×10^9 and 2.2×10^9 respectively (HBEFA 3.3, 2019). In Figure 7b, the
377 relative contributions of kilometers driven by Swedish Euro 0 to Euro VI HDTs are shown. Zhang et al. (2014) reported no
378 statistically significant difference in fuel consumption among Euro II to Euro IV buses under a real-world typical bus driving
379 cycle in Beijing. In this study, we assume the fuel consumption per kilometre and fuel density are the same across the different
380 Euro class HDTs and adopting the average fuel-based EFs calculated in this study (Tables 1 and 2), the approximation of
381 contributions of pollutants emitted from Swedish HDTs in each Euro class to the total PM, PN, BC and NO_x emissions are
382 depicted in Fig. 7c-f. Due to a lack of corresponding emission information, pollutant average EFs of Euro 0, Euro I and Euro
383 II HDTs were assumed to be at the same level as those of Euro III HDTs representing lower bound estimates. Euro 0-II HDTs
384 accounted for less than 2.2% of the grand total distance driven but totally contributed to 16%, 13%, 6% and 4% of BC, PM,
385 NO_x, and PN emissions. Euro III HDTs only accounted for 5% (Fig. 7b) of the total fleet but disproportionately contributed to
386 37%, 30%, 16% and 10% of BC, PM, NO_x, and PN emissions. Euro IV HDTs also exhibited disproportionately high PM and
387 NO_x emissions. A fraction of 32% of HDTs belonged to the Euro V category, they contributed to 53%, 42%, 34%, and 32%
388 of NO_x, PM, BC and PN emissions respectively. Upgrading, replacing or making obsolete Euro 0 to Euro V HDTs would be



389 necessary for mitigating a large part of the PM, PN, BC and NO_x emissions. Euro VI HDTs accounted for the highest fraction
390 of the total fleet (53%), but only contributed to 2%, 6%, 12% and 47% of PM, BC, NO_x, and PN emissions, indicating
391 successful overall pollution reduction with the introduction of more Euro VI HDVs. Using the median EFs as references, the
392 emission contributions from Euro VI HDTs to the total pollutant emissions would be even lower (Fig. S10). These data provide
393 useful information to predict future pollutant emission trends and to guide policy analysis and implementation. Since the
394 predicted transition in emissions from road transport would be significant, chemical transport model/cost-assessment models
395 need to get fast access to emission factors for new generation HDTs to be able to provide a better estimation of near future air
396 pollution levels.

397 **4 Atmospheric implications and conclusions**

398 The transition in the atmospheric emission of particles and gases from on-road HDTs caused by the modernisation of the fleet
399 is reported in this study. Particle emissions of PM, BC and to a lesser extent PN exhibited substantial reductions from Euro III
400 to Euro VI HDTs. The gaseous emissions of NO_x and CO also showed significant decrease with respect to Euro class, while
401 the HC emission was relatively low for all the HDT Euro class types. Compared with Euro III HDTs, Euro VI HDTs showed
402 99%, 98%, 93% and 57% reductions of the average emissions factors of PM, BC, NO_x, and CO respectively. Although a
403 significant reduction in NO_x emissions and a lower median EF_{NO₂} were evident, the fraction of NO₂ in the NO_x emissions
404 increased continuously from Euro IV to Euro VI HDTs, and Euro VI HDTs were the dominant class of the top 3% emitters
405 for NO₂. PN showed the largest data scattering for Euro VI HDTs, though after evaporation of the volatile fraction, SPN
406 became less scattered. A plausible reason for this large variability in PN but not PM is the formation of nucleation mode
407 particles containing more volatile compounds, which is more sensitive to individual driving and plume dilution conditions.

408 Driving condition and engine technology affected the size distribution of particle number emissions. The average particle
409 number size distributions of Euro III to EEV HDTs were bimodal with nucleation modes at ~6-10 nm and accumulation modes
410 at ~50-80 nm. Euro VI HDTs displayed nucleation mode dominant size distributions. Measurements of particle volatility
411 revealed that Euro VI HDTs had the highest volatile fraction in both nucleation mode and accumulation mode compared to the
412 other Euro classes. More detailed chemical composition information of this volatile fraction is needed to assess their potential
413 impacts for health and formation of SOA.

414 We also found that a small number of high emitters contributed to a large fraction of the total emissions. The top 10%
415 emitters in each pollutant category were responsible for 65% of total PM, 70% of total PN, 44% of total NO_x and 69% of total
416 NO₂ emissions, respectively. Euro III HDTs were the dominant top 3% emitters for PM and BC emissions, and Euro VI HDTs
417 were the dominant top 3% emitters for PN and NO₂ emissions.

418 In general, an overall pollution reduction has been achieved during the last years and the transition to Euro VI adoption
419 will take real-world on-road emissions into a new era of much lower contributions to air pollution. The emissions of PM, BC
420 and NO_x are predicted to further decrease in the future, while PN emissions may be subject to greater fluctuation and therefore



421 be more challenging to control. Upgrading or phasing-out of existing Euro 0 to Euro V vehicles and introducing more Euro VI
422 HDTs would result in large pollution reductions. More intensive attentions need to be focused on SPN controls for Euro VI
423 HDTs. A careful and more detailed examination of the impacts of fleet upgrades in terms of ambient pollutant levels and
424 emission reduction targets for individual pollutants may be needed for further evaluation.

425

426 *Data availability.*

427 The data used in this publication are available to the community and can be accessed by request to the corresponding author.

428 *Author contributions.*

429 ÅMH designed the project; LZ, ÅMH, CMS, SMG, ÅS, MJ, HS, MH, and IW conducted the measurements; LZ, CMS, and
430 QL analysed data; LZ, ÅMH, MH, CKC and BPL wrote the paper. All co-authors contributed to the discussion of the
431 manuscript.

432 *Competing interests.*

433 The authors declare that they have no conflict of interest.

434 *Acknowledgments.*

435 This work was financed by Formas (214-2013-1430) and was an initiative within the framework programme “Photochemical
436 smog in China” financed by the Swedish Research Council (639-2013-6917). Chak K. Chan would like to acknowledge the
437 support of the Science Technology and Innovation Committee of Shenzhen Municipality (project no.
438 JCYJ20160401095857424).

439

440 **References**

441 Alfoldy, B., Giechaskiel, B., Hofmann, W., and Drossinos, Y.: Size-distribution dependent lung deposition of diesel exhaust
442 particles, *J. Aerosol Sci.*, 40, 652-663, 10.1016/j.jaerosci.2009.04.009, 2009.

443 Amanatidis, S., Ntziachristos, L., Karjalainen, P., Saukko, E., Simonen, P., Kuittinen, N., Aakko-Saksa, P., Timonen, H.,
444 Ronkko, T., and Keskinen, J.: Comparative performance of a thermal denuder and a catalytic stripper in sampling laboratory
445 and marine exhaust aerosols, *Aerosol Sci. Tech.*, 52, 420-432, <https://doi.org/10.1080/02786826.2017.1422236>, 2018.

446 Arnold, F., Pirjola, L., Ronkko, T., Reichl, U., Schlager, H., Lahde, T., Heikkila, J., and Keskinen, J.: First online
447 measurements of sulfuric acid gas in modern heavy-duty diesel engine exhaust: implications for nanoparticle formation,
448 *Environ. Sci. Technol.*, 46, 11227-11234, <https://doi.org/10.1021/es302432s>, 2012.

449 Ban-Weiss, G. A., Lunden, M. M., Kirchstetter, T. W., and Harley, R. A.: Measurement of black carbon and particle number
450 emission factors from individual heavy-duty trucks, *Environ. Sci. Technol.*, 43, 1419-1424, <https://doi.org/10.1021/es8021039>,
451 2009.



- 452 Bergmann, M., Kirchner, U., Vogt, R., and Benter, T.: On-road and laboratory investigation of low-level PM emissions of a
453 modern diesel particulate filter equipped diesel passenger car, *Atmos. Environ.*, 43, 1908-1916,
454 <https://doi.org/10.1016/j.atmosenv.2008.12.039>, 2009.
- 455 Bishop, G. A., and Stedman, D. H.: A decade of on-road emissions measurements, *Environ. Sci. Technol.*, 42, 1651-1656,
456 <https://doi.org/10.1021/es702413b>, 2008.
- 457 Bishop, G. A., Peddle, A. M., Stedman, D. H., and Zhan, T.: On-road emission measurements of reactive nitrogen compounds
458 from three California cities, *Environ. Sci. Technol.*, 44, 3616-3620, <https://doi.org/10.1021/es903722p>, 2010.
- 459 Bishop, G. A., Schuchmann, B. G., and Stedman, D. H.: Heavy-duty truck emissions in the South Coast Air Basin of California,
460 *Environ. Sci. Technol.*, 47, 9523-9529, <https://doi.org/10.1021/es401487b>, 2013.
- 461 Bishop, G. A., Hottor-Raguindin, R., Stedman, D. H., McClintock, P., Theobald, E., Johnson, J. D., Lee, D. W., Zietsman, J.,
462 and Misra, C.: On-road heavy-duty vehicle emissions monitoring system, *Environ. Sci. Technol.*, 49, 1639-1645,
463 <https://doi.org/10.1021/es505534e>, 2015.
- 464 Biswas, S., Verma, V., Schauer, J. J., Cassee, F. R., Cho, A. K., and Sioutas, C.: Oxidative potential of semi-volatile and non-
465 volatile particulate matter (PM) from heavy-duty vehicles retrofitted with emission control technologies, *Environ. Sci.*
466 *Technol.*, 43, 3905-3912, <https://doi.org/10.1021/es9000592>, 2009.
- 467 Bocchi, C., Bazzini, C., Fontana, F., Pinto, G., Martino, A., and Cassoni, F.: Characterization of urban aerosol: seasonal
468 variation of mutagenicity and genotoxicity of PM_{2.5}, PM₁ and semi-volatile organic compounds, *Mutat. Res.*, 809, 16-23,
469 <https://doi.org/10.1016/j.mrgentox.2016.07.007>, 2016.
- 470 Burgard, D. A., Bishop, G. A., Stedman, D. H., Gessner, V. H., and Daeschlein, C.: Remote sensing of in-use heavy-duty
471 diesel trucks, *Environ. Sci. Technol.*, 40, 6938-6942, <https://doi.org/10.1021/es060989a>, 2006.
- 472 Burgard, D. A., and Provinsal, M. N.: On-road, in-use gaseous emission measurements by remote sensing of school buses
473 equipped with diesel oxidation catalysts and diesel particulate filters, *J. Air Waste Manag. Assoc.*, 59, 1468-1473,
474 <https://doi.org/10.3155/1047-3289.59.12.1468>, 2009.
- 475 Campagnolo, D., Cattaneo, A., Corbella, L., Borghi, F., Del Buono, L., Rovelli, S., Spinazze, A., and Cavallo, D. M.: In-
476 vehicle airborne fine and ultra-fine particulate matter exposure: The impact of leading vehicle emissions, *Environ. Int.*, 123,
477 407-416, <https://doi.org/10.1016/j.envint.2018.12.020>, 2019.
- 478 Carslaw, D. C., Beevers, S. D., Tate, J. E., Westmoreland, E. J., and Williams, M. L.: Recent evidence concerning higher NO_x
479 emissions from passenger cars and light-duty vehicles, *Atmos. Environ.*, 45, 7053-7063,
480 <https://doi.org/10.1016/j.atmosenv.2011.09.063>, 2011.
- 481 Carslaw, D. C., and Rhys-Tyler, G.: New insights from comprehensive on-road measurements of NO_x, NO₂ and NH₃ from
482 vehicle emission remote sensing in London, UK, *Atmos. Environ.*, 81, 339-347,
483 <https://doi.org/10.1016/j.atmosenv.2013.09.026>, 2013.
- 484 Carslaw, D. C., Farren, N. J., Vaughan, A. R., Drysdale, W. S., Young, S., and Lee, J. D.: The diminishing importance of
485 nitrogen dioxide emissions from road vehicle exhaust, *Atmospheric Environment: X*, 1, 100002,
486 <https://doi.org/10.1016/j.aeaoa.2018.100002>, 2019.
- 487 Chen, L., Wang, Z., Liu, S., and Qu, L.: Using a chassis dynamometer to determine the influencing factors for the emissions
488 of Euro VI vehicles, *Transport. Res. D- Tr. E.*, 65, 564-573, <https://doi.org/10.1016/j.trd.2018.09.022>, 2018.



- 489 Cheung, H. H. Y., Tan, H. B., Xu, H. B., Li, F., Wu, C., Yu, J. Z., and Chan, C. K.: Measurements of non-volatile aerosols
490 with a VTDMA and their correlations with carbonaceous aerosols in Guangzhou, China, *Atmos.*
491 *Chem. Phys.*, 16, 8431-8446, <https://doi.org/10.5194/acp-16-8431-2016>, 2016.
- 492 Clark, N. N., Gautam, M., Rapp, B. L., Lyons, D. W., Graboski, M. S., McCormick, R. L., Alleman, T. L., and Norton, P.:
493 Diesel and CNG transit bus emissions characterization by two chassis dynamometer laboratories: Results and issues, SAE
494 Technical Paper, 0148-7191, 1999.
- 495 Cui, M., Chen, Y. J., Feng, Y. L., Li, C., Zheng, J. Y., Tian, C. G., Yan, C. Q., and Zheng, M.: Measurement of PM and its
496 chemical composition in real-world emissions from non-road and on-road diesel vehicles, *Atmos.*
497 *Chem. Phys.*, 17, 6779-6795, <https://doi.org/10.5194/acp-17-6779-2017>, 2017.
- 498 Dallmann, T. R., DeMartini, S. J., Kirchstetter, T. W., Herndon, S. C., Onasch, T. B., Wood, E. C., and Harley, R. A.: On-road
499 measurement of gas and particle-phase pollutant emission factors for individual heavy-duty diesel trucks, *Environ. Sci.*
500 *Technol.*, 46, 8511-8518, <https://doi.org/10.1021/es301936c>, 2012.
- 501 Donahue, N. M., Robinson, A. L., Stanier, C. O., and Pandis, S. N.: Coupled partitioning, dilution, and chemical aging of
502 semivolatile organics, *Environ. Sci. Technol.*, 40, 2635-2643, <https://doi.org/10.1021/es052297c>, 2006.
- 503 Dreher, D. B., and Harley, R. A.: A fuel-based inventory for heavy-duty diesel truck emissions, *J. Air Waste Manage.*, 48,
504 352-358, <https://doi.org/10.1080/10473289.1998.10463686>, 1998.
- 505 Du, Y., Xu, X., Chu, M., Guo, Y., and Wang, J.: Air particulate matter and cardiovascular disease: the epidemiological,
506 biomedical and clinical evidence, *J. Thorac. Dis.*, 8, E8-E19, <http://dx.doi.org/10.3978/j.issn.2072-1439.2015.11.37> 2016.
- 507 Edwards, R., Larivé, J., Rieckard, D., and Weindorf, W.: Well-to-Wheels analysis of future automotive fuels and powertrains
508 in the European context: Well-to-Tank Appendix 2-Version 4a, Joint Research Centre of the European Commission, EUCAR,
509 and CONCAWE, 1-133, <http://10.2790/95629>, 2014.
- 510 EEA: Air Quality in Europe - 2018 Report, 2018.
- 511 Franco, V., Kousoulidou, M., Muntean, M., Ntziachristos, L., Hausberger, S., and Dilara, P.: Road vehicle emission factors
512 development: A review, *Atmos. Environ.*, 70, 84-97, <https://doi.org/10.1016/j.atmosenv.2013.01.006>, 2013.
- 513 Gentner, D. R., Jathar, S. H., Gordon, T. D., Bahreini, R., Day, D. A., El Haddad, I., Hayes, P. L., Pieber, S. M., Platt, S. M.,
514 de Gouw, J., Goldstein, A. H., Harley, R. A., Jimenez, J. L., Prevot, A. S., and Robinson, A. L.: Review of Urban Secondary
515 Organic Aerosol Formation from Gasoline and Diesel Motor Vehicle Emissions, *Environ. Sci. Technol.*, 51, 1074-1093,
516 <https://doi.org/10.1021/acs.est.6b04509>, 2017.
- 517 Gertler, A. W.: Diesel vs. gasoline emissions: Does PM from diesel or gasoline vehicles dominate in the US?, *Atmos. Environ.*,
518 39, 2349-2355, <https://doi.org/10.1016/j.atmosenv.2004.05.065>, 2005.
- 519 Giechaskiel, B., Alföldy, B., and Drossinos, Y.: A metric for health effects studies of diesel exhaust particles, *J. Aerosol Sci.*,
520 40, 639-651, <https://doi.org/10.1016/j.jaerosci.2009.04.008>, 2009.
- 521 Giechaskiel, B., Mamakos, A., Andersson, J., Dilara, P., Martini, G., Schindler, W., and Bergmann, A.: Measurement of
522 Automotive Nonvolatile Particle Number Emissions within the European Legislative Framework: A Review, *Aerosol Sci.*
523 *Tech.*, 46, 719-749, <https://doi.org/10.1080/02786826.2012.661103>, 2012.



- 524 Giechaskiel, B., Schwelberger, M., Delacroix, C., Marchetti, M., Feijen, M., Prieger, K., Andersson, S., and Karlsson, H. L.:
525 Experimental assessment of solid particle number Portable Emissions Measurement Systems (PEMS) for heavy-duty vehicles
526 applications, *J. Aerosol Sci.*, 123, 161-170, <https://doi.org/10.1016/j.jaerosci.2018.06.014>, 2018.
- 527 Gkatzelis, G. I., Papanastasiou, D. K., Florou, K., Kaltsonoudis, C., Louvaris, E., and Pandis, S. N.: Measurement of
528 nonvolatile particle number size distribution, *Atmos. Meas. Tech.*, 9, 103-114, <https://doi.org/10.5194/amt-9-103-2016>, 2016.
- 529 The climate policy framework: <http://www.government.se/articles/2017/06/the-climate-policy-framework/>, 2017.
- 530 Grigoratos, T., Fontaras, G., Giechaskiel, B., and Zacharof, N.: Real-world emissions performance of heavy-duty Euro VI
531 diesel vehicles, *Atmos. Environ.*, 201, 348-359, <https://doi.org/10.1016/j.atmosenv.2018.12.042>, 2019.
- 532 Guo, J. D., Ge, Y. S., Hao, L. J., Tan, J. W., Li, J. Q., and Feng, X. Y.: On-road measurement of regulated pollutants from
533 diesel and CNG buses with urea selective catalytic reduction systems, *Atmos. Environ.*, 99, 1-9,
534 <https://doi.org/10.1016/j.atmosenv.2014.07.032>, 2014.
- 535 Hak, C. S., Hallquist, M., Ljungstrom, E., Svane, M., and Pettersson, J. B. C.: A new approach to in-situ determination of
536 roadside particle emission factors of individual vehicles under conventional driving conditions, *Atmos. Environ.*, 43, 2481-
537 2488, <https://doi.org/10.1016/j.atmosenv.2009.01.041>, 2009.
- 538 Hallquist, A. M., Jerksjo, M., Fallgren, H., Westerlund, J., and Sjodin, A.: Particle and gaseous emissions from individual
539 diesel and CNG buses, *Atmos. Chem. Phys.*, 13, 5337-5350, <https://doi.org/10.5194/acp-13-5337-2013>, 2013.
- 540 Hallquist, M., Wenger, J. C., Baltensperger, U., Rudich, Y., Simpson, D., Claeys, M., Dommen, J., Donahue, N. M., George,
541 C., Goldstein, A. H., Hamilton, J. F., Herrmann, H., Hoffmann, T., Iinuma, Y., Jang, M., Jenkin, M. E., Jimenez, J. L., Kiendler-
542 Scharr, A., Maenhaut, W., McFiggans, G., Mentel, T. F., Monod, A., Prevot, A. S. H., Seinfeld, J. H., Surratt, J. D., Szmigielski,
543 R., and Wildt, J.: The formation, properties and impact of secondary organic aerosol: current and emerging issues, *Atmos.*
544 *Chem. Phys.*, 9, 5155-5236, <https://doi.org/10.5194/acp-9-5155-2009>, 2009.
- 545 Haugen, M. J., Bishop, G. A., Thiruvengadam, A., and Carder, D. K.: Evaluation of Heavy-and Medium-Duty On-Road
546 Vehicle Emissions in California's South Coast Air Basin, *Environ. Sci. Technol.*, 52, 13298-13305,
547 <https://doi.org/10.1021/acs.est.8b03994>, 2018.
- 548 He, C., Li, J., Ma, Z., Tan, J., and Zhao, L.: High NO₂/NO_x emissions downstream of the catalytic diesel particulate filter: An
549 influencing factor study, *J. Environ. Sci. (China)*, 35, 55-61, <https://doi.org/10.1016/j.jes.2015.02.009>, 2015.
- 550 He, L., Hu, J., Zhang, S., Wu, Y., Guo, X., Guo, X., Song, J., Zu, L., Zheng, X., and Bao, X.: Investigating real-world emissions
551 of China's heavy-duty diesel trucks: Can SCR effectively mitigate NO_x emissions for highway trucks, *Aerosol Air. Qual. Res.*,
552 17, 2585-2594, <https://DOI: 10.4209/aaqr.2016.12.0531>, 2017.
- 553 Heeb, N. V., Schmid, P., Kohler, M., Gujer, E., Zennegg, M., Wenger, D., Wichser, A., Ulrich, A., Gfeller, U., Honegger, P.,
554 Zeyer, K., Emmenegger, L., Petermann, J. L., Czerwinski, J., Mosimann, T., Kasper, M., and Mayer, A.: Impact of low- and
555 high-oxidation diesel particulate filters on genotoxic exhaust constituents, *Environ. Sci. Technol.*, 44, 1078-1084,
556 <https://doi.org/10.1021/es9019222>, 2010.
- 557 Herner, J. D., Hu, S., Robertson, W. H., Huai, T., Collins, J. F., Dwyer, H., and Ayala, A.: Effect of advanced aftertreatment
558 for PM and NO_x control on heavy-duty diesel truck emissions, *Environ. Sci. Technol.*, 43, 5928-5933,
559 <https://doi.org/10.1021/es9008294>, 2009.



- 560 Herner, J. D., Hu, S., Robertson, W. H., Huai, T., Chang, M.-C. O., Rieger, P., and Ayala, A.: Effect of advanced aftertreatment
561 for PM and NO_x reduction on heavy-duty diesel engine ultrafine particle emissions, *Environ. Sci. Technol.*, 45, 2413-2419,
562 <https://doi.org/10.1021/es102792y>, 2011.
- 563 Heywood, J. B.: *Internal combustion engine fundamentals*, 1988.
- 564 Huffman, J. A., Ziemann, P. J., Jayne, J. T., Worsnop, D. R., and Jimenez, J. L.: Development and characterization of a fast-
565 stepping/scanning thermodenuder for chemically-resolved aerosol volatility measurements, *Aerosol Sci. Tech.*, 42, 395-407,
566 <https://doi.org/10.1080/02786820802104981>, 2008.
- 567 Janhall, S., and Hallquist, M.: A novel method for determination of size-resolved, submicrometer particle traffic emission
568 factors, *Environ. Sci. Technol.*, 39, 7609-7615, <https://doi.org/10.1021/es048208y>, 2005.
- 569 Jarvinen, A., Timonen, H., Karjalainen, P., Bloss, M., Simonen, P., Saarikoski, S., Kuuluvainen, H., Kalliokoski, J., Dal Maso,
570 M., Niemi, J. V., Keskinen, J., and Ronkko, T.: Particle emissions of Euro VI, EEV and retrofitted EEV city buses in real
571 traffic, *Environ. Pollut.*, 250, 708-716, <https://doi.org/10.1016/j.envpol.2019.04.033>, 2019.
- 572 Jiang, Y., Yang, J., Cocker, D., 3rd, Karavalakis, G., Johnson, K. C., and Durbin, T. D.: Characterizing emission rates of
573 regulated pollutants from model year 2012+ heavy-duty diesel vehicles equipped with DPF and SCR systems, *Sci. Total
574 Environ.*, 619-620, 765-771, <https://doi.org/10.1016/j.scitotenv.2017.11.120>, 2018.
- 575 Kittelson, D., Watts, W., and Johnson, J.: *Diesel Aerosol Sampling Methodology—CRC E-43*, Final report, Coordinating
576 Research Council, 2002.
- 577 Ko, J., Myung, C. L., and Park, S.: Impacts of ambient temperature, DPF regeneration, and traffic congestion on NO_x emissions
578 from a Euro 6-compliant diesel vehicle equipped with an LNT under real-world driving conditions, *Atmos. Environ.*, 200, 1-
579 14, <https://doi.org/10.1016/j.atmosenv.2018.11.029>, 2019.
- 580 Kousoulidou, M., Ntziachristos, L., Mellios, G., and Samaras, Z.: Road-transport emission projections to 2020 in European
581 urban environments, *Atmos. Environ.*, 42, 7465-7475, <https://doi.org/10.1016/j.atmosenv.2008.06.002>, 2008.
- 582 Kozawa, K. H., Park, S. S., Mara, S. L., and Herner, J. D.: Verifying emission reductions from heavy-duty diesel trucks
583 operating on Southern California freeways, *Environ. Sci. Technol.*, 48, 1475-1483, <https://doi.org/10.1021/es4044177>, 2014.
- 584 Lau, C. F., Rakowska, A., Townsend, T., Brimblecombe, P., Chan, T. L., Yam, Y. S., Mocnik, G., and Ning, Z.: Evaluation
585 of diesel fleet emissions and control policies from plume chasing measurements of on-road vehicles, *Atmos. Environ.*, 122,
586 171-182, <https://doi.org/10.1016/j.atmosenv.2015.09.048>, 2015.
- 587 Le Breton, M., Psichoudaki, M., Hallquist, M., Watne, Å., Lutz, A., and Hallquist, Å.: Application of a FIGAERO ToF CIMS
588 for on-line characterization of real-world fresh and aged particle emissions from buses, *Aerosol Sci. Tech.*, 1-16,
589 <https://doi.org/10.1080/02786826.2019.1566592>, 2019.
- 590 Lee, B. H., Lopez-Hilfiker, F. D., Mohr, C., Kurten, T., Worsnop, D. R., and Thornton, J. A.: An iodide-adduct high-resolution
591 time-of-flight chemical-ionization mass spectrometer: application to atmospheric inorganic and organic compounds, *Environ.
592 Sci. Technol.*, 48, 6309-6317, <https://doi.org/10.1021/es500362a>, 2014.
- 593 Li, X., Dallmann, T. R., May, A. A., Stanier, C. O., Grieshop, A. P., Lipsky, E. M., Robinson, A. L., and Presto, A. A.: Size
594 distribution of vehicle emitted primary particles measured in a traffic tunnel, *Atmos. Environ.*, 191, 9-18,
595 <https://doi.org/10.1016/j.atmosenv.2018.07.052>, 2018.



- 596 Liu, Q., Hallquist, Å. M., Fallgren, H., Jerksjö, M., Jutterström, S., Salberg, H., Hallquist, M., Le Breton, M., Pei, X., and
597 Pathak, R. K.: Roadside assessment of a modern city bus fleet: Gaseous and particle emissions, *Atmospheric Environment: X*,
598 100044, <https://doi.org/10.1016/j.aeaoa.2019.100044>, 2019.
- 599 Liu, Z. G., Vasys, V. N., Dettmann, M. E., Schauer, J. J., Kittelson, D. B., and Swanson, J.: Comparison of Strategies for the
600 Measurement of Mass Emissions from Diesel Engines Emitting Ultra-Low Levels of Particulate Matter, *Aerosol Sci. Tech.*,
601 43, 1142-1152, <https://doi.org/10.1080/02786820903219035>, 2009.
- 602 Lv, Y., Li, X., Xu, T. T., Cheng, T. T., Yang, X., Chen, J. M., Iinuma, Y., and Herrmann, H.: Size distributions of polycyclic
603 aromatic hydrocarbons in urban atmosphere: sorption mechanism and source contributions to respiratory deposition, *Atmos.*
604 *Chem. Phys.*, 16, 2971-2983, <https://doi.org/10.5194/acp-16-2971-2016>, 2016.
- 605 Mahmoudzadeh Andwari, A., Pesiridis, A., Esfahanian, V., Salavati-Zadeh, A., Karvountzis-Kontakiotis, A., and
606 Muralidharan, V.: A comparative study of the effect of turbo compounding and ORC waste heat recovery systems on the
607 performance of a turbocharged heavy-duty diesel engine, *Energies*, 10, 1087, <https://doi.org/10.3390/en10081087>, 2017.
- 608 Manigrasso, M., Vernale, C., and Avino, P.: Traffic aerosol lobar doses deposited in the human respiratory system, *Environ.*
609 *Sci. Pollut. Res. Int.*, 24, 13866-13873, <https://doi.org/10.1007/s11356-015-5666-1>, 2017.
- 610 Maricq, M. M., and Ning, X.: The effective density and fractal dimension of soot particles from premixed flames and motor
611 vehicle exhaust, *J. Aerosol Sci.*, 35, 1251-1274, <https://doi.org/10.1016/j.jaerosci.2004.05.002>, 2004.
- 612 Maricq, M. M.: Chemical characterization of particulate emissions from diesel engines: A review, *J. Aerosol Sci.*, 38, 1079-
613 1118, <https://doi.org/10.1016/j.jaerosci.2007.08.001>, 2007.
- 614 Martinet, S., Liu, Y., Louis, C., Tassel, P., Perret, P., Chaumond, A., and Andre, M.: Euro 6 Unregulated Pollutant
615 Characterization and Statistical Analysis of After-Treatment Device and Driving-Condition Impact on Recent Passenger-Car
616 Emissions, *Environ. Sci. Technol.*, 51, 5847-5855, <https://doi.org/10.1021/acs.est.7b00481>, 2017.
- 617 Martini, G., Giechaskiel, B., and Dilara, P.: Future European emission standards for vehicles: the importance of the UN-ECE
618 Particle Measurement Programme, *Biomarkers*, 14 Suppl 1, 29-33, <https://doi.org/10.1080/13547500902965393>, 2009.
- 619 May, A. A., Nguyen, N. T., Presto, A. A., Gordon, T. D., Lipsky, E. M., Karve, M., Gutierrez, A., Robertson, W. H., Zhang,
620 M., Brandow, C., Chang, O., Chen, S. Y., Cicero-Fernandez, P., Dinkins, L., Fuentes, M., Huang, S. M., Ling, R., Long, J.,
621 Maddox, C., Massetti, J., McCauley, E., Miguel, A., Na, K., Ong, R., Pang, Y. B., Rieger, P., Sax, T., Truong, T., Vo, T.,
622 Chattopadhyay, S., Maldonado, H., Maricq, M. M., and Robinson, A. L.: Gas- and particle-phase primary emissions from in-
623 use, on-road gasoline and diesel vehicles, *Atmos. Environ.*, 88, 247-260, <https://doi.org/10.1016/j.atmosenv.2014.01.046>,
624 2014.
- 625 Mendoza-Villafuerte, P., Suarez-Bertoa, R., Giechaskiel, B., Riccobono, F., Bulgheroni, C., Astorga, C., and Perujo, A.: NO_x,
626 NH₃, N₂O and PN real driving emissions from a Euro VI heavy-duty vehicle. Impact of regulatory on-road test conditions on
627 emissions, *Sci. Total Environ.*, 609, 546-555, <https://doi.org/10.1016/j.scitotenv.2017.07.168>, 2017.
- 628 Moody, A., and Tate, J.: In Service CO₂ and NO_x Emissions of Euro 6/VI Cars, Light-and Heavy-dutygoods Vehicles in Real
629 London driving: Taking the Road into the Laboratory, *Journal of Earth Sciences and Geotechnical Engineering*, 7, 51-62,
630 <https://orcid.org/0000-0003-1646-6852>, 2017.
- 631 Nelson, P. F., Tibbett, A. R., and Day, S. J.: Effects of vehicle type and fuel quality on real-world toxic emissions from diesel
632 vehicles, *Atmos. Environ.*, 42, 5291-5303, <https://doi.org/10.1016/j.atmosenv.2008.02.049>, 2008.



- 633 Pirjola, L., Dittrich, A., Niemi, J. V., Saarikoski, S., Timonen, H., Kuuluvainen, H., Jarvinen, A., Kousa, A., Ronkko, T., and
634 Hillamo, R.: Physical and Chemical Characterization of Real-World Particle Number and Mass Emissions from City Buses in
635 Finland, *Environ. Sci. Technol.*, 50, 294-304, <https://doi.org/10.1021/acs.est.5b04105>, 2016.
- 636 Pirjola, L., Niemi, J. V., Saarikoski, S., Aurela, M., Enroth, J., Carbone, S., Saarnio, K., Kuuluvainen, H., Kousa, A., Ronkko,
637 T., and Hillamo, R.: Physical and chemical characterization of urban winter-time aerosols by mobile measurements in Helsinki,
638 Finland, *Atmos. Environ.*, 158, 60-75, <https://doi.org/10.1016/j.atmosenv.2017.03.028>, 2017.
- 639 Preble, C., Cados, T., Harley, R., and Kirchstetter, T.: Impacts of Aging Emission Control Systems on In-Use Heavy-Duty
640 Diesel Truck Emission Rates, AGU Fall Meeting Abstracts, 2017,
- 641 Preble, C. V., Dallmann, T. R., Kreisberg, N. M., Hering, S. V., Harley, R. A., and Kirchstetter, T. W.: Effects of Particle
642 Filters and Selective Catalytic Reduction on Heavy-Duty Diesel Drayage Truck Emissions at the Port of Oakland, *Environ.*
643 *Sci. Technol.*, 49, 8864-8871, <https://doi.org/10.1021/acs.est.5b01117>, 2015.
- 644 Preble, C. V., Cados, T. E., Harley, R. A., and Kirchstetter, T. W.: In-Use Performance and Durability of Particle Filters on
645 Heavy-Duty Diesel Trucks, *Environ. Sci. Technol.*, 52, 11913-11921, <https://doi.org/10.1021/acs.est.8b02977>, 2018.
- 646 Quiros, D. C., Hu, S. H., Hu, S. S., Lee, E. S., Sardar, S., Wang, X. L., Olfert, J. S., Jung, H. J. S., Zhu, Y. F., and Huai, T.:
647 Particle effective density and mass during steady-state operation of GDI, PFI, and diesel passenger cars, *J. Aerosol Sci.*, 83,
648 39-54, <https://doi.org/10.1016/j.jaerosci.2014.12.004>, 2015.
- 649 Quiros, D. C., Thiruvengadam, A., Pradhan, S., Besch, M., Thiruvengadam, P., Demirgok, B., Carder, D., Oshinuga, A., Huai,
650 T., and Hu, S.: Real-world emissions from modern heavy-duty diesel, natural gas, and hybrid diesel trucks operating along
651 major California freight corridors, *Emission Control Science and Technology*, 2, 156-172, [https://doi.org/10.1007/s40825-](https://doi.org/10.1007/s40825-016-0044-0)
652 016-0044-0, 2016.
- 653 Quiros, D. C., Smith, J. D., Ham, W. A., Robertson, W. H., Huai, T., Ayala, A., and Hu, S.: Deriving fuel-based emission
654 factor thresholds to interpret heavy-duty vehicle roadside plume measurements, *J. Air Waste Manag. Assoc.*, 68, 969-987,
655 <https://doi.org/10.1080/10962247.2018.1460637>, 2018.
- 656 Rexeis, M., Röck, M., and Hausberger, S.: Comparison of Fuel Consumption and Emissions for Representative Heavy-Duty
657 Vehicles in Europe, 2018.
- 658 Ristimäki, J., Vaaraslahti, K., Lappi, M., and Keskinen, J.: Hydrocarbon condensation in heavy-duty diesel exhaust, *Environ.*
659 *Sci. Technol.*, 41, 6397-6402, <https://doi.org/10.1021/es0624319>, 2007.
- 660 Robinson, A. L., Donahue, N. M., Shrivastava, M. K., Weitkamp, E. A., Sage, A. M., Grieshop, A. P., Lane, T. E., Pierce, J.
661 R., and Pandis, S. N.: Rethinking organic aerosols: semivolatile emissions and photochemical aging, *Science*, 315, 1259-1262,
662 <https://doi.org/10.1126/science.1133061>, 2007.
- 663 Rymaniak, L., Ziolkowski, A., and Gallas, D.: Particle number and particulate mass emissions of heavy-duty vehicles in real
664 operating conditions, *MATEC Web of Conferences*, 2017, 00025,
- 665 Sakurai, H., Park, K., McMurry, P. H., Zarling, D. D., Kittelson, D. B., and Ziemann, P. J.: Size-dependent mixing
666 characteristics of volatile and nonvolatile components in diesel exhaust aerosols, *Environ. Sci. Technol.*, 37, 5487-5495,
667 <https://doi.org/10.1021/es034362t>, 2003a.



- 668 Sakurai, H., Tobias, H. J., Park, K., Zarling, D., Docherty, K. S., Kittelson, D. B., McMurry, P. H., and Ziemann, P. J.: On-
669 line measurements of diesel nanoparticle composition and volatility, *Atmos. Environ.*, 37, 1199-1210,
670 [https://doi.org/10.1016/S1352-2310\(02\)01017-8](https://doi.org/10.1016/S1352-2310(02)01017-8), 2003b.
- 671 Smit, R., Keramydas, C., Ntziachristos, L., Lo, T. S., Ng, K. L., Wong, H. L. A., and Wong, C.: Evaluation of real-world
672 gaseous emissions performance of SCR and DPF bus retrofits, *Environ. Sci. Technol.*, <https://doi.org/10.1021/acs.est.8b07223>,
673 2019.
- 674 Tan, Y., Henderick, P., Yoon, S., Herner, J., Montes, T., Boriboonsomsin, K., Johnson, K., Scora, G., Sandez, D., and Durbin,
675 T. D.: On-Board Sensor-Based NO_x Emissions from Heavy-Duty Diesel Vehicles, *Environ. Sci. Technol.*, 53, 5504-5511,
676 <https://doi.org/10.1021/acs.est.8b07048>, 2019.
- 677 Thiruvengadam, A., Besch, M. C., Carder, D. K., Oshinuga, A., and Gautam, M.: Influence of real-world engine load
678 conditions on nanoparticle emissions from a DPF and SCR equipped heavy-duty diesel engine, *Environ. Sci. Technol.*, 46,
679 1907-1913, <https://doi.org/10.1021/es203079n>, 2012.
- 680 Thiruvengadam, A., Besch, M. C., Thiruvengadam, P., Pradhan, S., Carder, D., Kappanna, H., Gautam, M., Oshinuga, A.,
681 Hogo, H., and Miyasato, M.: Emission rates of regulated pollutants from current technology heavy-duty diesel and natural gas
682 goods movement vehicles, *Environ. Sci. Technol.*, 49, 5236-5244, <https://doi.org/10.1021/acs.est.5b00943>, 2015.
- 683 Vaaraslahti, K., Virtanen, A., Ristimäki, J., and Keskinen, J.: Nucleation mode formation in heavy-duty diesel exhaust with
684 and without a particulate filter, *Environ. Sci. Technol.*, 38, 4884-4890, <https://doi.org/10.1021/es0353255>, 2004.
- 685 Van Setten, B. A., Makkee, M., and Moulijn, J. A.: Science and technology of catalytic diesel particulate filters, *Catalysis*
686 *Reviews*, 43, 489-564, <https://doi.org/10.1081/CR-120001810>, 2001.
- 687 Vojtisek-Lom, M., Pechout, M., Dittrich, L., Beranek, V., Kotek, M., Schwarz, J., Vodicka, P., Milcova, A., Rossnerova, A.,
688 Ambroz, A., and Topinka, J.: Polycyclic aromatic hydrocarbons (PAH) and their genotoxicity in exhaust emissions from a
689 diesel engine during extended low-load operation on diesel and biodiesel fuels, *Atmos. Environ.*, 109, 9-18,
690 <https://doi.org/10.1016/j.atmosenv.2015.02.077>, 2015.
- 691 Wang, T., Quiros, D. C., Thiruvengadam, A., Pradhan, S., Hu, S., Huai, T., Lee, E. S., and Zhu, Y.: Total Particle Number
692 Emissions from Modern Diesel, Natural Gas, and Hybrid Heavy-Duty Vehicles During On-Road Operation, *Environ. Sci.*
693 *Technol.*, 51, 6990-6998, <https://doi.org/10.1021/acs.est.6b06464>, 2017.
- 694 Watne, A. K., Psichoudaki, M., Ljungstrom, E., Le Breton, M., Hallquist, M., Jerksjo, M., Fallgren, H., Jutterstrom, S., and
695 Hallquist, A. M.: Fresh and Oxidized Emissions from In-Use Transit Buses Running on Diesel, Biodiesel, and CNG, *Environ.*
696 *Sci. Technol.*, 52, 7720-7728, <https://doi.org/10.1021/acs.est.8b01394>, 2018.
- 697 Williams, M., and Minjares, R.: A technical summary of Euro 6/VI vehicle emission standards, International Council for Clean
698 Transportation (ICCT), Washington, DC, accessed July, 10, 2017, 2016.
- 699 Zavala, M., Molina, L. T., Yacovitch, T. I., Fortner, E. C., Roscioli, J. R., Floerchinger, C., Herndon, S. C., Kolb, C. E.,
700 Knighton, W. B., Paramo, V. H., Zirath, S., Mejia, J. A., and Jazcilevich, A.: Emission factors of black carbon and co-pollutants
701 from diesel vehicles in Mexico City, *Atmos. Chem. Phys.*, 17, 15293-15305, <https://doi.org/10.5194/acp-17-15293-2017>,
702 2017.
- 703 Zhang, S. J., Wu, Y., Liu, H., Huang, R. K., Yang, L. H. Z., Li, Z. H., Fu, L. X., and Hao, J. M.: Real-world fuel consumption
704 and CO₂ emissions of urban public buses in Beijing, *Appl. Energ.*, 113, 1645-1655,
705 <https://doi.org/10.1016/j.apenergy.2013.09.017>, 2014.



- 706 Zheng, Z., Johnson, K. C., Liu, Z., Durbin, T. D., Hu, S., Huai, T., Kittelson, D. B., and Jung, H. S.: Investigation of solid
707 particle number measurement: Existence and nature of sub-23 nm particles under PMP methodology, *J. Aerosol Sci.*, 42, 883-
708 897, <https://doi.org/10.1016/j.jaerosci.2011.08.003>, 2011.
- 709 Zheng, Z., Durbin, T. D., Xue, J., Johnson, K. C., Li, Y., Hu, S., Huai, T., Ayala, A., Kittelson, D. B., and Jung, H. S.:
710 Comparison of particle mass and solid particle number (SPN) emissions from a heavy-duty diesel vehicle under on-road driving
711 conditions and a standard testing cycle, *Environ. Sci. Technol.*, 48, 1779-1786, <https://doi.org/10.1021/es403578b>, 2014.
- 712 Zheng, Z. Q., Durbin, T. D., Karavalakis, G., Johnson, K. C., Chaudhary, A., Cocker, D. R., Herner, J. D., Robertson, W. H.,
713 Huai, T., Ayala, A., Kittelson, D. B., and Jung, H. S.: Nature of Sub-23-nm Particles Downstream of the European Particle
714 Measurement Programme (PMP)-Compliant System: A Real-Time Data Perspective, *Aerosol Sci. Tech.*, 46, 886-896,
715 <https://doi.org/10.1080/02786826.2012.679167>, 2012.
- 716 Zhu, Y. F., Hinds, W. C., Kim, S., Shen, S., and Sioutas, C.: Study of ultrafine particles near a major highway with heavy-duty
717 diesel traffic, *Atmos. Environ.*, 36, 4323-4335, [https://doi.org/10.1016/S1352-2310\(02\)00354-0](https://doi.org/10.1016/S1352-2310(02)00354-0), 2002.



718 **Table 1.** Comparison of the average emission data^a for PM and PN from the present study with literature data.

PM/PN						
Vehicle type	Speed km h ⁻¹	Dp range nm	Method	Instrument	EF _{PM} mg (kg fuel) ⁻¹	EF _{PN} # (kg fuel) ⁻¹ 10 ¹⁴
Euro III HDT in this study	26±6 ^b	5.6-560	roadside	EEPS	684±365	20.3±11.7
Euro III bus (Hallquist et al., 2013)	acceleration	5.6-560	roadside	EEPS	6.7-2074	0.11-45
	constant speed	5.6-560	roadside	EEPS	151-273	0.12-4.2
Euro III bus with DPF (Hallquist et al., 2013)	acceleration	5.6-560	roadside	EEPS	62-2465	1.9-23
	constant speed	5.6-560	roadside	EEPS	41-142	1.1-9.7
Euro III bus (Pirjola et al., 2016)	≤25 (bus depot)	PM ₁ D _p ≥2.5	plume chasing	ELPI ^c CPC	1240±220 ^b	20.6±3.2 ^b
	≤45 (bus line)	PM ₁ D _p ≥2.5	plume chasing	ELPI ^c CPC	500	17.7
	acceleration	5.6-560	roadside	EEPS	8.9±0.2	0.12±0.12
Euro III bus with DPF+SCR (Watne et al., 2018)	stop and go (bus stop)	5.6-560	roadside	EEPS	30±26 ^b	14.0±3.0 ^b
Euro III diesel bus and truck (Zavala et al., 2017)	driving cycle	35-1000	plume chasing & roadside	SP-AMS ^f	4300	-
Euro IV HDT in this study	23±8 ^b	5.6-560	roadside	EEPS	172±68	8.7±3.0
Euro IV bus with EGR (Hallquist et al., 2013)	acceleration	5.6-560	roadside	EEPS	562-3089	13-44
	constant speed	5.6-560	roadside	EEPS	91-489	5.8-47
Euro IV bus with EGR+DPF (Hallquist et al., 2013)	acceleration	5.6-560	roadside	EEPS	177-650	5.1-13
	constant speed	5.6-560	roadside	EEPS	58-61	2.6-3.1
Euro IV bus with EGR+DPF (Pirjola et al., 2016)	≤25 (bus depot)	PM ₁ D _p ≥2.5	plume chasing	ELPI ^c CPC	1190±520 ^b	8.9±1.6 ^b
	acceleration	5.6-560	roadside	EEPS	145-560	3-13
Euro IV diesel bus and truck (Zavala et al., 2017)	driving cycle	35-1000	plume chasing and roadside	SP-AMS ^f	1800	-
Euro V HDT in this study	27±7 ^b	5.6-560	roadside	EEPS	146±49	9.7±2.7
Euro V bus+SCR (Hallquist et al., 2013)	acceleration	5.6-560	roadside	EEPS	125-766	4.4-92
	constant speed	5.6-560	roadside	EEPS	41-509	2.7-33
Euro V bus (Watne et al., 2018)	acceleration	5.6-560	roadside	EEPS	145±70	3.0±1.7
Euro V HDV with SCR (Rymaniak et al., 2017)	average at 45	PM/ 5.6-560	PEMS	MSS ^c EEPS	1840 ^d	0.09 ^d
	stop and go (bus stop)	5.6-560	roadside	EEPS	180±15 ^b	6.5±2.9 ^b
Euro V diesel bus and truck (Zavala et al., 2017)	driving cycle	35-1000	plume chasing and roadside	SP-AMS ^f	720	-
EEV HDT in this study	25±8 ^b	5.6-560	roadside	EEPS	78±35	16.5±23.6



EEV bus with EGR +DPF (Pirjola et al., 2016)	≤25 (bus depot)	PM ₁ / D _p ≥2.5	plume chasing	ELPI ^c CPC	400±280 ^b	2.1±0.1 ^b
EEV bus with SCR (Pirjola et al., 2016)	≤25 (bus depot)	PM ₁ / D _p ≥2.5	plume chasing	ELPI ^c CPC	280±170 ^b	7.0±3.8 ^b
EEV with DOC+DPF+SCR (Rymaniak et al., 2017)	average at 45	PM/ 5.6-560	PEMS	MSS ^e EEPS	236 ^d	0.02 ^d
EEV bus (Jarvinen et al., 2019)	stop and go	PM ₁ / D _p ≥3	plume chasing	ELPI ^c CPC	200	8.6
Euro VI HDT in this study	29±8 ^b	5.6-560	roadside	EEPS	5±2	8.5±4.6
Euro VI bus (Jarvinen et al., 2019)	stop and go	PM ₁ / D _p ≥3	plume chasing	ELPI ^c CPC	70	5
Euro VI HDGV (Moody and Tate, 2017)	13-86	-	PEMS	-	28-33 ^d	-
Euro VI HDT (Grigoratos et al., 2019)	65-74	-	PEMS	-	-	0.002-0.01 ^d
HDV with DPF (Wang et al., 2017; Quiros et al., 2016)	13-80	PM D _p ≥5	PEMS	gravimetric CPC	12-41 ^d	0.006-13.2
Heavy-duty HDV with DPF+SCR (Thiruvengadam et al., 2015)	driving cycle	PM	chassis dynamometer	gravimetric	6-29 ^d	-
HDV with DPF+SCR (Jiang et al., 2018)	driving cycle	PM _{2.5}	chassis dynamometer	gravimetric	3-97 ^d	-
HDT (model year 2004- 2006) (Preble et al., 2015)	accelerating or cruise at 48	D _p ≥2.5	roadside	CPC	-	47.2±9.7
HDT with SCR+DPF (model year 2010- 2013) (Preble et al., 2015)	48	D _p ≥2.5	roadside	CPC	-	15.9±11.5
HDV (mean model year 2005) (Bishop et al., 2015)	15.7-16.8	PM _{1,2}	OHMS ^g	digital mass monitor	650	-
HDV (mean model year 2009) (Bishop et al., 2015)	7.7-9.3	PM _{1,2}	OHMS ^g	digital mass monitor	31	-
HDV without after-treatment (Quiros et al., 2018)	driving cycle	PM _{2.5}	chassis dynamometer	gravimetric	1980 ^d	-
HDV+DPF (Quiros et al., 2018)	driving cycle	PM _{2.5}	chassis dynamometer	gravimetric	6-9 ^d	-
HDT without available Euro type information	27±7 ^b	5.6-560	roadside	EEPS	47±23	7.5±7.3
Total Swedish HDT	28±7 ^b	5.6-560	roadside	EEPS	96±36	9.6±2.7
Total non-Swedish HDT	26±8 ^b	5.6-560	roadside	EEPS	117±42	11.1±4.2

719 ^a Given errors are at 95% CI.

720 ^b Standard deviation.

721 ^c ELPI, Electrical Low-Pressure Impactor.

722 ^d Average fuel consumption of 0.26 L km⁻¹ for HDV during long haul and regional delivery tests (Rexeis et al., 2018), the
 723 density of 0.815 kg dm⁻³ (Swedish Environmental Protection Agency, 2013) of diesel particles were assumed for unit
 724 conversion.

725 ^e MSS, Micro Soot Sensor.



726 ^f SP-AMS, Soot Particle Aerosol Mass Spectrometer.
727 ^g OHMS, On-Road Heavy-Duty Vehicle Emissions Monitoring System.



728 **Table 2.** Comparison of the average emission data^a for NO_x, NO₂/NO_x, CO and HC from the present study with literature data.

Vehicle type	Speed km h ⁻¹	Method	EF _{NO_x} ^b g (kg fuel) ⁻¹	EF _{NO₂} / EF _{NO_x} ^b mass ratio %	EF _{CO} ^c g (kg fuel) ⁻¹	EF _{HC} ^c g (kg fuel) ⁻¹
Euro III HDT in this study	26±6 ^d	roadside	43.3±31.5	7.5±4.1	36.0±13.2	0.8±1.3
Euro III bus (Hallquist et al., 2013)	acceleration	roadside	16.1±9.7	-	16.1±16.1	<13
Euro III bus (Pirjola et al., 2016)	≤25 (bus depot)	plume chasing	12.7±1.8 ^d	-	-	-
	≤45 (bus line)	plume chasing	20.5	-	-	-
Euro III bus with DPF+SCR (Watne et al., 2018)	acceleration	roadside	-	-	13±10	0.02
Euro III HDV (Lau et al., 2015)	64 ± 13 ^d	plume chasing	-	24±4	-	-
Euro III & IV HDV (Kousoulidou et al., 2008)	-	model	-	14	-	-
Euro III HGV (Carslaw et al., 2011)	Average at 31	roadside	16.2±1.0 ^f	-	-	-
Euro IV HDT in this study	23±8 ^d	roadside	19.8±10.1	2.7±2.9	22.1±10.3	0.7±1.1
Euro IV bus (Hallquist et al., 2013)	acceleration	roadside	12.9±6.5	-	16.1±16.1	<13
Euro IV bus with EGR+DPF (Pirjola et al., 2016)	≤25 (bus depot)	plume chasing	23.4±6.1 ^d	-	-	-
Euro IV bus with SCR (Watne et al., 2018)	roadside	acceleration	-	-	220-230	0.3-0.6
Euro IV HDV (Lau et al., 2015)	64 ± 13 ^d	plume chasing	-	28±5	-	-
Euro IV HGV (Carslaw et al., 2011)	average at 31	roadside	10.3±1.4 ^f	-	-	-
Euro V HDT in this study	27±7 ^d	roadside	22.2±3.8	6.0±2.8	22.8±5.1	0.9±0.4
Euro V bus (Hallquist et al., 2013)	acceleration	roadside	35.5±9.7	-	9.7±3.2	<13
Euro V bus with SCR (Liu et al., 2019)	stop and go (bus stop)	roadside	9.8±3.5 ^d	3.7±1.5 ^d	28 ^e	2.2 ^e
Euro V HDV (Lau et al., 2015)	64 ± 13 ^d	plume chasing	-	40±14	-	-
Euro V HDV (Kousoulidou et al., 2008)	-	model	-	18	-	-
Euro V HGV (Carslaw et al., 2011)	average at 31	roadside	13.3±5.8 ^f	-	-	-
EEV HDT in this study	25±8 ^d	roadside	13.6±6.7	6.3±3.7	18.0±10.1	0.2±0.4
EEV bus with EGR +DPF (Pirjola et al., 2016)	≤25 (bus depot)	plume chasing	32.9±7.6 ^d	-	-	-
EEV bus with SCR (Pirjola et al., 2016)	≤25 (bus depot)	plume chasing	39.8±4.2 ^d	-	-	-
Euro VI HDT in this study	29±8 ^d	roadside	3.1±1.0	22.5±4.2	15.5±2.2	1.0±0.5



Euro VI HDT (Grigoratos et al., 2019)	65-74	PEMS	0.3-31.3	-	2.8-22.3	0.3-3.1
Euro VI HDV (Kousoulidou et al., 2008)	-	model	-	35	-	-
Euro VI HDV (Moody and Tate, 2017)	driving cycle	PEMS	2.2 ^f	-	-	-
Heavy-duty HDV with DPF+SCR (Thiruvengadam et al., 2015)	driving cycle	chassis dynamometer	3.8-27.8 ^f	-	0.1-13.4 ^f	<0.64 ^f
HDV with DPF+SCR (Jiang et al., 2018)	driving cycle	chassis dynamometer	0.2-66.4 ^f	-	0.006- 14.9 ^f	<1.3 ^f
HDV with DOC+DPF+SCR (Quiros et al., 2016)	12.7-85.6	mobile laboratory	1.7-11.8 ^f	-	0.9-2.8 ^f	0.1-0.4 ^f
HDV (May et al., 2014)	driving cycle	chassis dynamometer	30-43	-	-	-
HDV with SCR (May et al., 2014)	driving cycle	chassis dynamometer	11	-	-	-
HDV fleet average (Haugen et al., 2018)	22.5±0.9	remote sensing	12.4±0.6	8.9	5.9±0.9	2.2±0.4
HDT (model year 2004- 2006) (Preble et al., 2015)	accelerating or cruise at 48	roadside	16.5±1.7	3.4±1.8	-	-
HDT with SCR+DPF (model year 2010- 2013) (Preble et al., 2015)	48	roadside	5.1±1.2	22.1±8.4	-	-
HDT (model year 2001) (Burgard et al., 2006)	5-25	roadside	-	9.1±0.5	26.0±2.1	1.8±0.6
HDT (model year 2000) (Burgard et al., 2006)	20-40	roadside	-	6.1±0.1	37.9±1.6	3.3±0.4
Fleet average in 2006 (Bishop and Stedman, 2008)	28-36	roadside	2-5	-	17-24	1.9-2.3
HDT fleet average (Dallmann et al., 2012)	65	roadside	28±1.5	7.0	8.0±1.2	-
HDT (mean model year 2004) (Bishop et al., 2013)	22.2±0.4	remote sensing	20.6±0.6 ^d	9.7	8.2±0.6 ^d	3.7±0.1 ^d
HDT (mean model year 2009) (Bishop et al., 2013)	7.8±0.1	remote sensing	19.9±0.3 ^d	9.0	7.3±0.5 ^d	0.6±0.6 ^d
HDT without available Euro type information	27±7 ^d	roadside	7.8±4.5	13.9±6.3	20.7±5.6	0.8±0.6
Total Swedish HDT	28±7 ^d	roadside	10.7±1.8	15.9±2.5	18.6±1.9	0.9±0.3
Total non-Swedish HDT	26±8 ^d	roadside	13.0±2.5	12.7±3.0	19.1±3.0	0.9±0.6

729 ^a Given errors are at 95% CI.

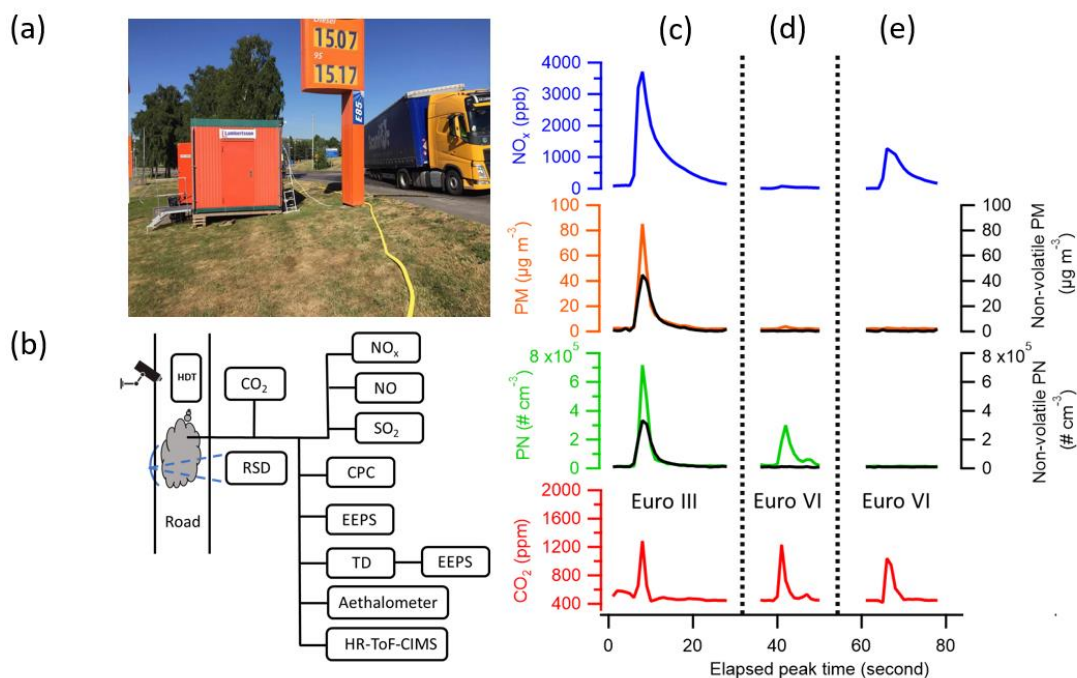
730 ^b In NO₂ equivalents.

731 ^c RSD data. For the RSD data sets of multiple individuals, negative values were replaced by zero when calculating the averages.

732 ^d Standard deviation.

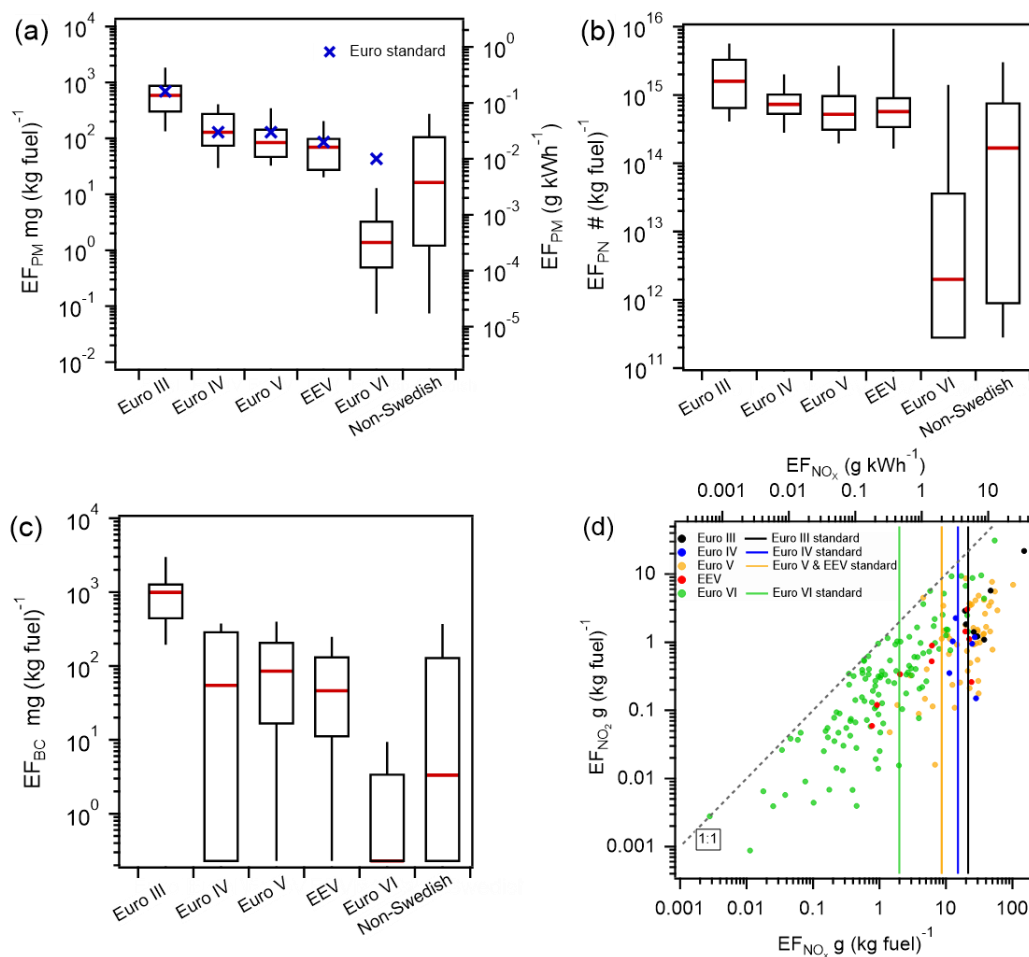
733 ^e Median.

734 ^f Average fuel consumption of 0.26 L km⁻¹ for HDV during long haul and regional delivery tests (Rexeis et al., 2018), the
 735 density of 0.815 kg dm⁻³ (Swedish Environmental Protection Agency, 2013) of diesel particles were assumed.

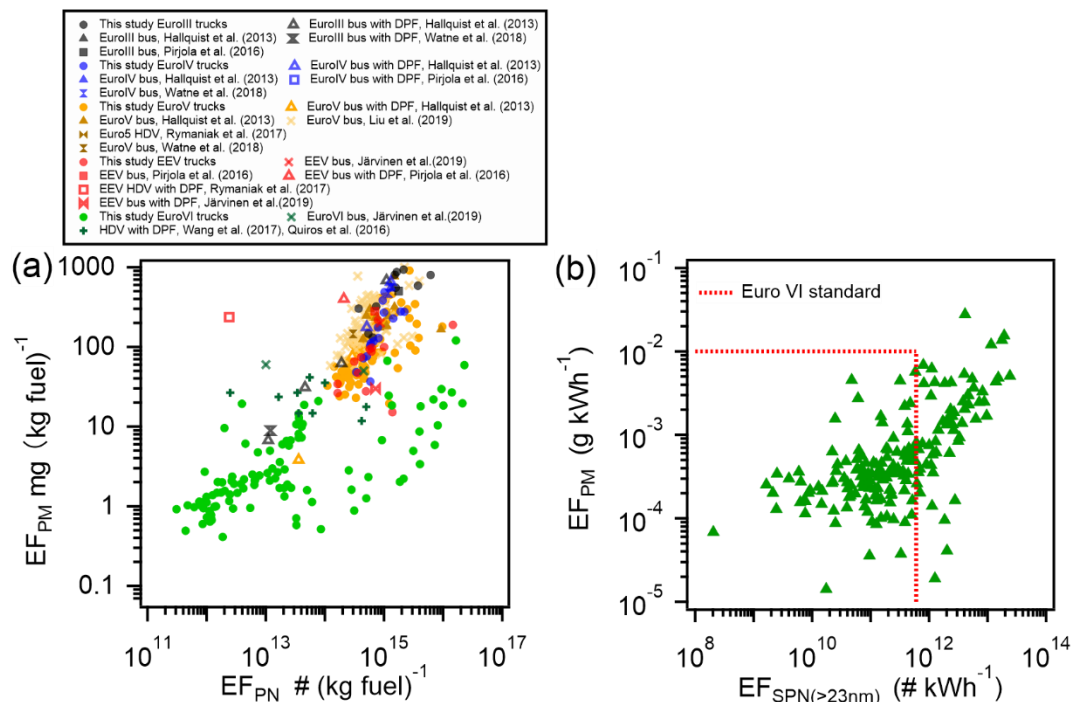


736

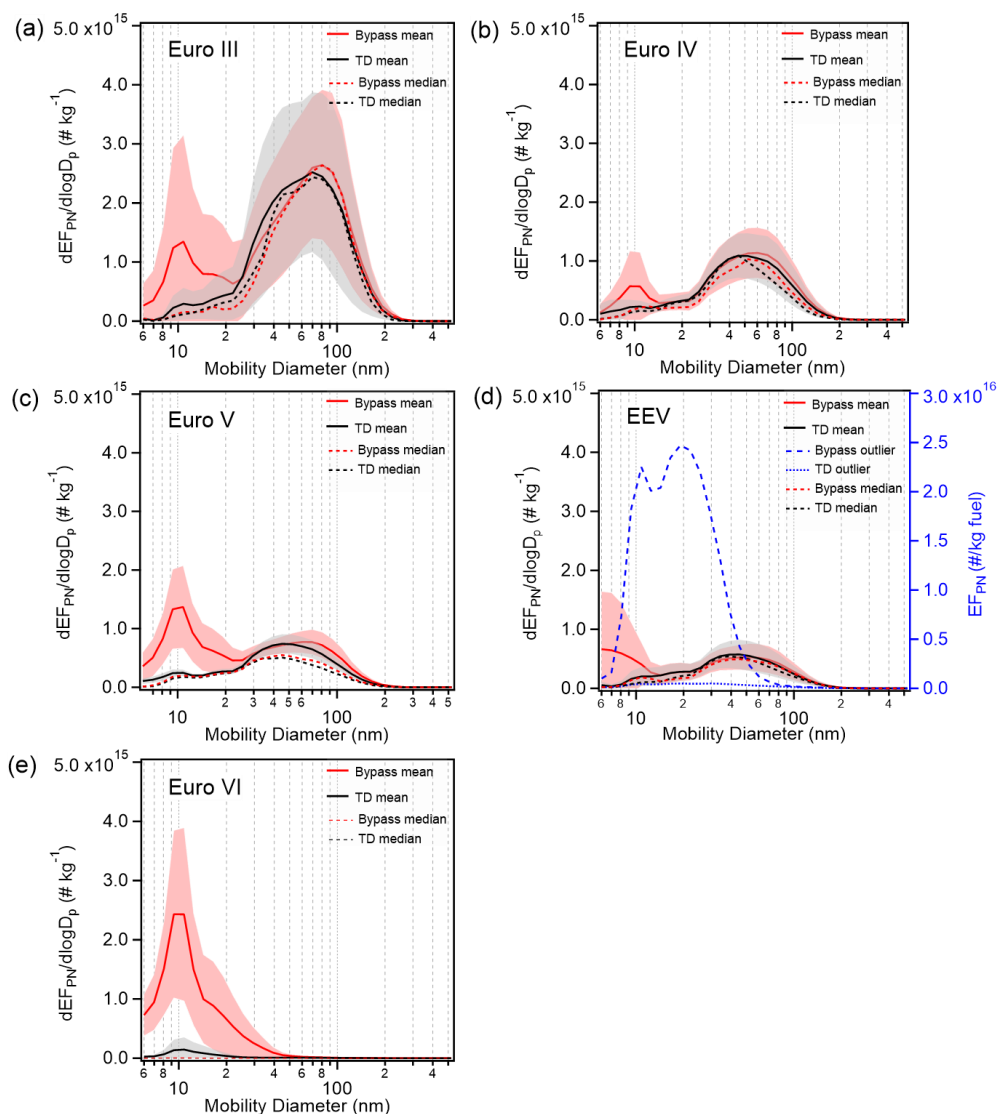
737 **Figure 1.** (a) Sampling site at the roadside in Gothenburg, Sweden, (b) schematic of the experimental set-up. HDT (Heavy-
738 duty truck), RSD (Remote Sensing Device), CPC (Condensation Particle Counter), EEPS (Engine Exhaust Particle Sizer
739 Spectrometer), TD (Thermodenuder) and HR-ToF-CIMS* (High-Resolution Time-of-Flight Chemical Ionization Mass
740 Spectrometer) and examples of signals from three passing HDTs. Concentrations of CO₂, PN, non-volatile PN, PM, non-
741 volatile PM, and NO_x from (c) a typical Euro III HDTs and (d) a typical Euro VI HDTs and (e) a Euro VI HDTs with low PN
742 emission. *The data from the HR-ToF-CIMS will be presented elsewhere.



743
744 **Figure 2.** (a) EF_{PM} , (b) EF_{PN} , (c) EF_{BC} , (d) EF_{NO_2} and EF_{NO_x} for Euro III to Euro VI and non-Swedish HDTs. Non-detectable
745 pollutant emission signals for captured plumes have been replaced by EF_{min} . For box-and-whisker plots, the top and the bottom
746 line of the box are 75th and 25th percentiles of the data, the red line inside the box is the median, and the top and bottom
747 whiskers are 90th and 10th percentiles. EF_{NO_x} in (d) are in NO_2 equivalents. Note that the comparison with the emission standard
748 is only indicative as they are based on test cycle performance.

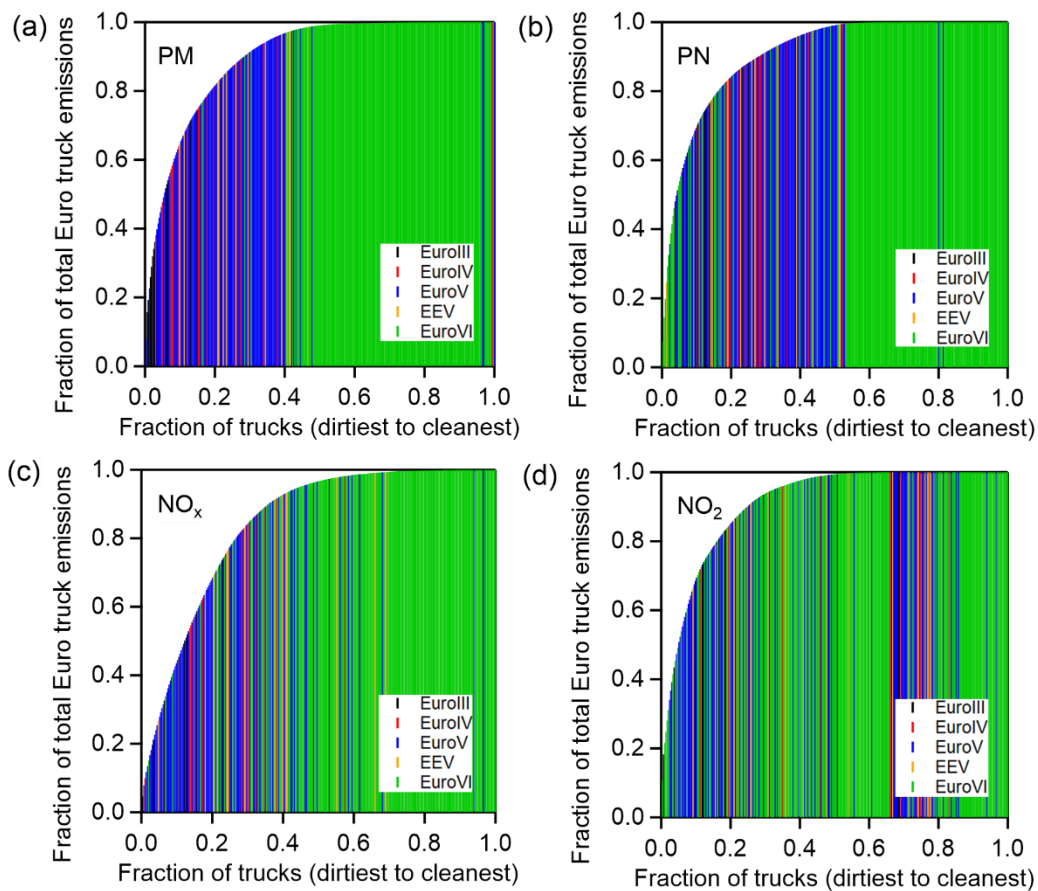


749
 750 **Figure 3.** (a) EF_{PM} and EF_{PN} of individual HDTs in this study and previous studies and (b) the relationship between EF_{PM} and
 751 EF_{SPN} of Euro VI HDTs. Red dashed lines represent Euro emission standards (horizontal: PM emission standard; vertical: SPN
 752 emission standard). Note that the comparison with the emission standard is only indicative as they are based on test cycle
 753 performance.



754

755 **Figure 4.** Mean and median size-resolved EF_{PN} and $EF_{non-volatile\ PN}$ of different Euro class HDTs. Shaded regions in (a-e)
756 represent the statistical 95% confidence interval. One HDT with extremely different EF in (d) was excluded and shown in
757 blue.

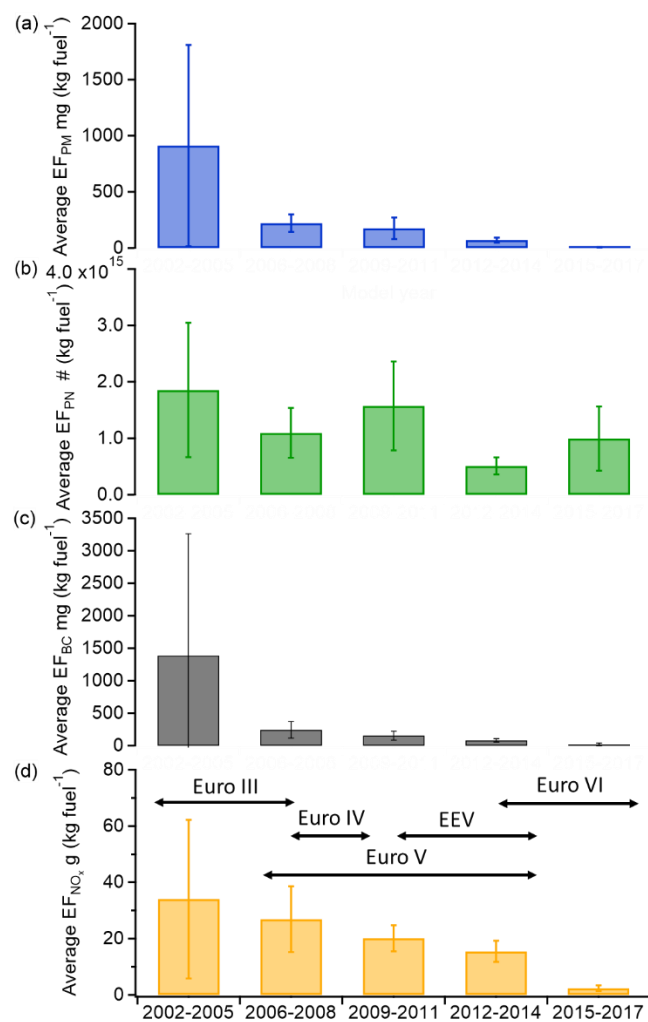


758

759

760

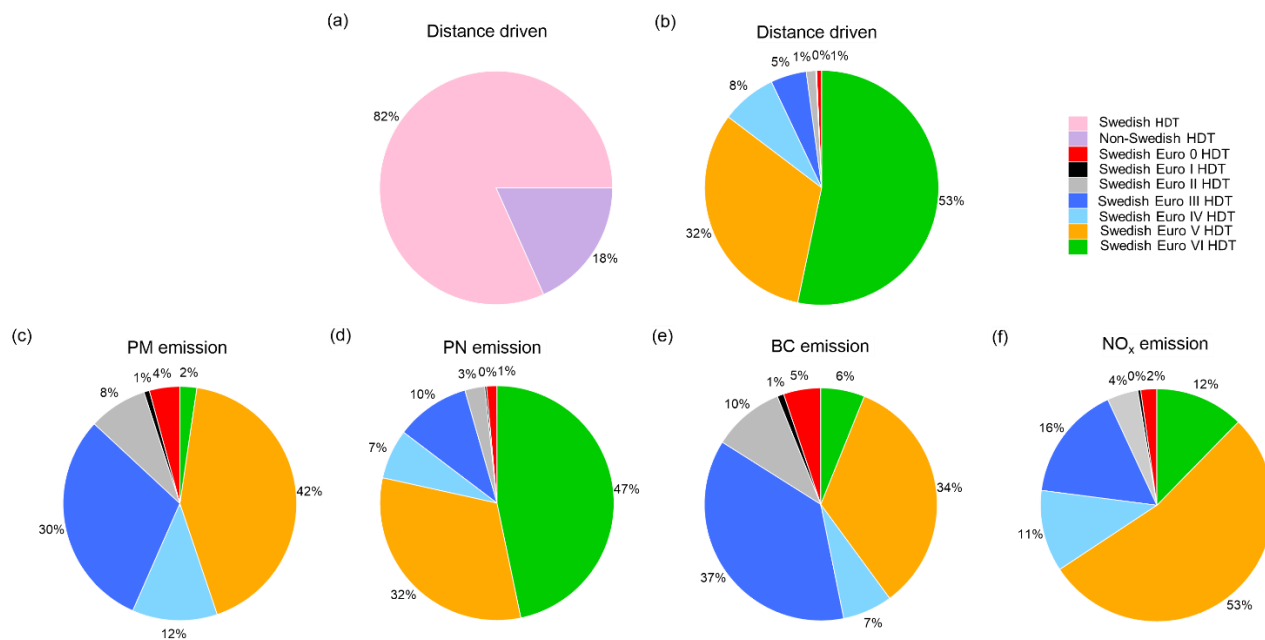
Figure 5. Cumulative emission factor distribution for (a) PM, (b) PN, (c) NO_x, and (d) NO₂ measured in HDT exhaust plumes with HDTs ranked from the highest to lowest in terms of emission factors.



761

762 **Figure 6.** Changes of average EFs of (a) PM, (b) PN, (c) BC and (d) NO_x with respect to the registration year of HDTs. Error
 763 bars represent the statistical 95% confidence interval. Black arrows mark the years that the particular type of HDT examined
 764 in this study was first registered.

765



766
767 **Figure 7.** Relative contributions of kilometers driven by (a) Swedish and Non-Swedish HDTs and (b) Swedish Euro 0, Euro
768 I, Euro II, Euro III, Euro IV, Euro V and Euro VI HDTs on Swedish roads during 2018. Approximation of contributions of
769 pollutants emitted from Swedish HDTs in each Euro class to the total (c) PM, (d) PN, (e) BC and (f) NO_x emissions.